UNIVERSITÀ DEGLI STUDI DI UDINE

CORSO DI DOTTORATO DI RICERCA IN SCIENZE BIOMEDICHE E BIOTECNOLOGICHE

XXVI CICLO
2013-2014

TESI DI DOTTORATO DI RICERCA

DISSECTION OF THE ROLE OF NG2/CSPG4 PROTEOGLYCAN IN TUMOR PROGRESSION

DOTTORANDO

Elisabetta Lombardi

RELATORE
Prof. Roberto Perris

CORRELATORI
Prof. Carlo Puccillo
Prof. Ivan De Curtis

to my family

SUMMARY

ABSTRACT

To accomplish the metastatic process, disseminating tumor cells enter haematic and lymphatic conduits to reach distant sites where they egress the circulation by penetrating the vessel wall – a phenomenon denoted extravasation and thought to involve complex interactions between the tumor cells, the vascular cells and their associated ECM. More recent experimental data suggest that pericytes may play a particularly critical role in this process, while a plephora of cell surface components present on all the interacting cell types are believed to act as promoters of transvascular passage. Cell surface proteoglycans (PGs) are among the components believed to be central cell membrane- and ECM-associated factors in this context, although it is not fully understood how they operate. The transmembrane proteoglycan NG2/CSPG4 is widely documented to be a tumor-promoting agent capable of driving tumor spread through the promotion of intricate microenvironmental interactions and is thereby is a prime candidate for the regulation of the cellular and molecular interactions underpinning the intra- and extravasation processes. The present thesis work has therefore approached the putative role of NG2/CSPG4 in the control of tumor spread, with specific reference to its potential ability to mediate the cancer cells' interaction with vascular structures. As starting point, the effectiveness of NG2/CSPG4 in promoting tumor growth in vitro and in vivo (xenogenic setting in athymic mice) was comparatively and quantitatively evaluated using a larger panel of melanoma, sarcoma and carcinoma cell lines with diverse, constitutive expression of NG2 and with immunosorted NG2/CSPG4-positive (representing putative cancer initiating cells) and NG2/CSPG4-negative subsets of some of these cancer cell lines. These experiments firmly corroborated the pro-tumorigenic role of NG2/CSPG4 and further highlighted its putative role in the control of cancer cell-host microenvironmental interplays. Global gene profiling evidenced marked gene expression differences between the two cell phenotypes, which are currently under investigation. Parallel antibody array-based phospho-proteomic analyses revealed NG2/CSPG4 phenotype-specific differences in the phosphorylation status of key molecules of the PI-3K and Rho/Rho-GAP pathways. The above cell types were then assayed under both static and shear-dependent conditions for their ability to interact with vascular cells and their matrices. To this end, a novel method for the in vitro derivation of native cell-

free ECMs was developed with the aim to obtain matrices reproducing in vitro the in vivo exhibited compositional and supramolecular configuration, as defined by in vivo metabolic labelling, immunochemistry and AFM and eSEM analyses. NG2/CSPG4-expressing cells responded to differently to matrices derived from immature perivascular cells and in particular motility responses further differed between NG/CSPG4+ and NG2/CSPG- cell subsets. Involvement of the proteoglycan in cell adhesion on different substrates was confirmed through the use of propriety functional-blocking anti-NG2/CSPG4 antibodies and by RNAi-mediated knockdown of the molecule. The potential involvement of NG2/CSPG4 in the process of extravasation was addressed by "static" transmigration assays involving monolayers of endothelial cells and smooth muscle cells and by experiments under flow. Both the core protein of the PG and its glycan chains were found to be involved in these cellular interactions. To finally address the NG2/CSPG4 function in the interaction between cancer cells and the luminal blood vessel wall and the impact of the proteoglycan in the passage of cancer cells through the vasculature, assays involving the chick embryo chorionallontoic membrane were exploited in combination with fluorescence real-time imaging. Again a substantial contribution of the proteoglycan in this process could be observed. The findings of the study contribute to our understanding of the pro-tumorigenic role of NG2/CSPG4 and lend support to the idea that the proteoglycan could play an active role in the control of the metastatic process. The observations therefore reinforce the value of NG2/CSPG4 as a therapeutic target and encourage a more detailed pre-clinical evaluation of the anti-NG2/CSPG4 examined in this study as therapeutic agents.

INTRODUCTION

METASTATIC PROCESS

Metastatis formation is a multistep cell-biological process involving dissemination of cancer cells to anatomically distant sites of the body and their subsequent adaptation to foreign tissue microenvironment[1,2,3,4]. Pro-metastatic cells dissociate from the primary tumor mass, thanks to a loss of cell-cell adhesion induced by down-regulation of cadherins and their cytoscheletal mediators, invade their surrounding extracellular matrix (ECM), approach the outer walls of lymphatic and haematic vessels, and frequently undergo transendothelial movement to enter circulation[5,6]. Thus, the metastatic process could be divided into five distinct phases: (1) loss of cell-cell junctions, detachment of cells from primary lesions and invasion of adjacent tissues; 2) intravasation; 3) navigation through body fluids; 4) extravasation; and 5) colonization of diverse tissue districts (Figure 1)

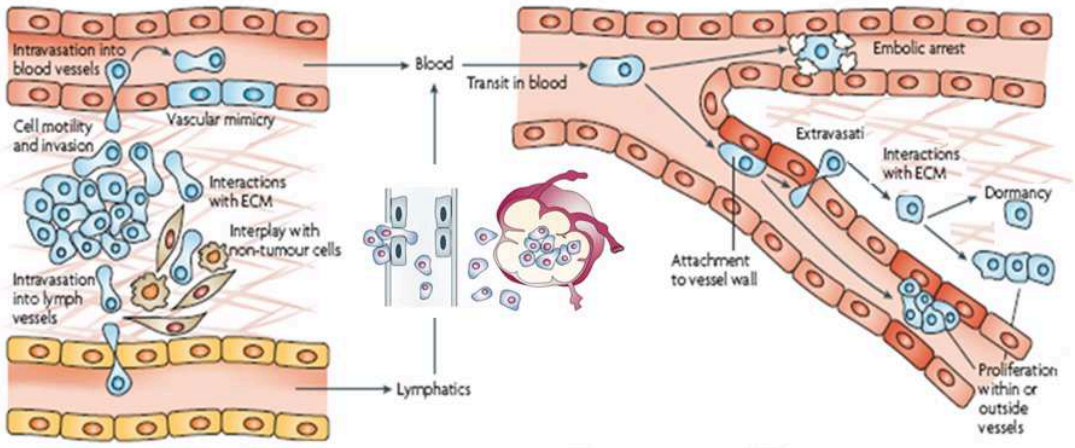

Figure 1 - **Schematic overview of the various facets of the metastatic process (adapted from Sahai et al., 2007).** Owing to the acquired ability of cancer cells to migrate through adjacent tissues and their associated ECM, in part promoted by the interactions with the microenvironment, pro-metastatic cells enter haematic and lymphatic vessels. Transendothelial migration is in this case brought about in the *intravasation* mode, allowing a certain number of cells composing the primary lesions to initiate their spreading through body fluids. Thus, this step is an obligatory one for setting the premises for the formation of distant secondary lesions. At defined sites, disseminating cancer cells may approach the luminal vessel wall and stabilize the contact with the endothelial cell surface. It is likely that this process is strongly favoured by the interaction of the disseminating cancer cells with platelets and leukocytes. At this point, cancer cells firmly attached to the endothelium may initiate singly the transendothelial movement or start propagating.

The process of tissue and ECM invasion preceding transendothelial movement is a highly dynamic process that requires complex and coordinated regulations of the extracellular interactions and cytoscheletal rearrangements[7,8]

(Figure 2). To migrate, the cell body must modify its shape and stiffness: at the beginning cell becomes roundish and in a second moment, when it moves, it becomes polarized and elongated. To move cells utilize cyoplasmic-membrane formations known as pseudopodia, lamellipoda and filopoda. All these structure are extension of the cell's leading edge and all contain filamentous actin, varying sets of intracellular structural and signalling proteins and a spectrum of cell surface-associated molecules probing the microenvironment. Collectively, these intra- and extracellular components are instrumental in the promotion of the local tractions forces that lead to the gradual forward gliding of the cell body and retraction of the trailing edge, while controlling the process of mechanotransduction.

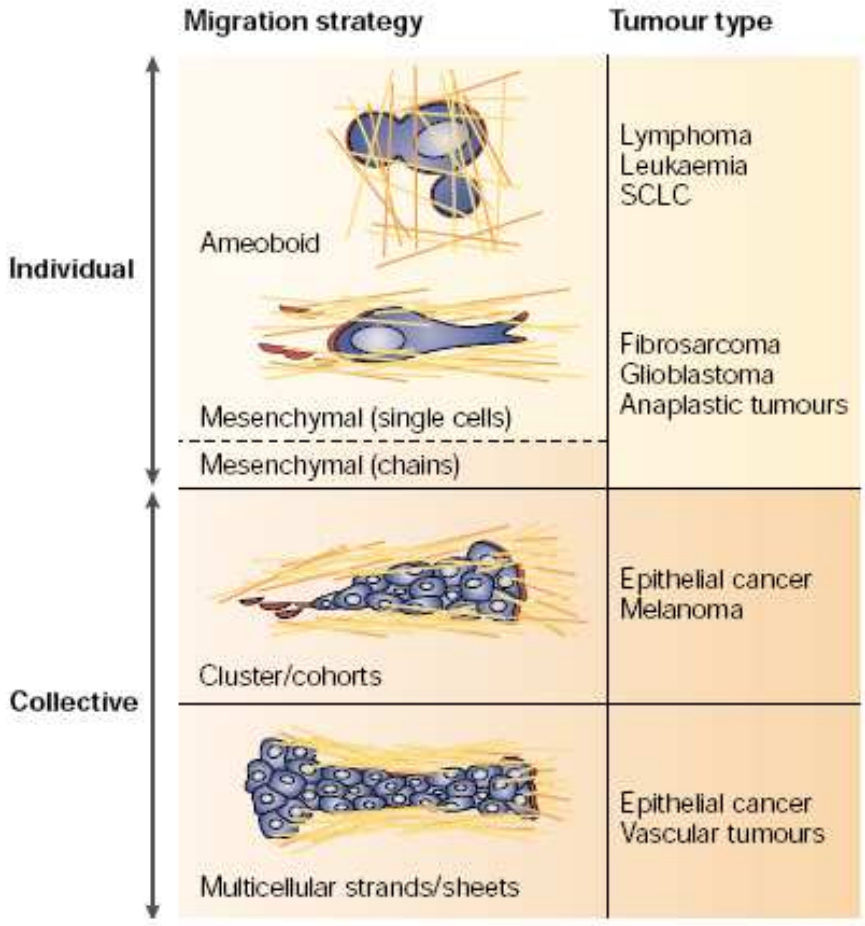

Figure 2 - **Modes of cell migration and invasion.** Different tumor types have been shown to use different strategies for migrating through tissues and ECMs and may move as individual cells or as entire populations (collective movement). Thus, malignant haematopoietic cells (leukaemia and lymphoma) and small-cell lung carcinoma (SCLC) cells are known to utlize an amoeboid movement, whereas sarcomas and glioblastomas move by a by a mesenchymal-type migration mode. Epithelial cancers move mostly as cohort and clusters of cells, whereas melanoma cells can adapt to the environment and switch between individual and collective migration (adapted from Friedl et. al, 2003)

Invasion through the stroma to reach the outer lining of blood vessels is likely to be promoted by the combination of soluble factors (chemotaxis), interstitial ECM components (haptotaxis) and interactions of the invading tumor cells with the surrounding cells, including infiltrating or resident tumor-associated macrophages. Once approaching the blood vessel lining, tumor cells would come in contact with pericytes, which are known to play a major role in the control of the intravasation process. Cancer cells can then enter the circulation by transmigrating either paracellularly through the endothelial cell junctions, or transcellularly through the endothelial cell body, as specifically demonstrated for the entrance of disseminating cancer cells through the lymphatic vessels. Degrading activity of MMP1 seems to be required for paracellular intravasation in regions where protease-activated receptor 1 (PAR1) on endothelial cells mediates the remodelling of endothelial junctions. Alternatively, ADAM12 of the endothelium can induce cleavage of VE-cadherin and the TIE2 receptor, which leads to disruption of endothelial junctions. TNF1α and TGFβ1 are two primary secretion products of invading cancer cells taking part in the induction of the retraction of endothelial junctions and thereby contributing to transendothelial migration. Cancer cells further take advantage of Notch receptors to bind to Notch ligands on the endothelium. During transcellular intravasation, the Ca^{2+} – activated calmodulin acts on MLCK of endothelial cells to cause actomyosin contraction through phosphorylation of myosin II at the sites of cancer cell attachmet. In turn, this leads to rapid cytoskeletal and membrane remodelling, which creates a transitory pore-like structure for the cancer cell to cross the endothelium (Figure 3).

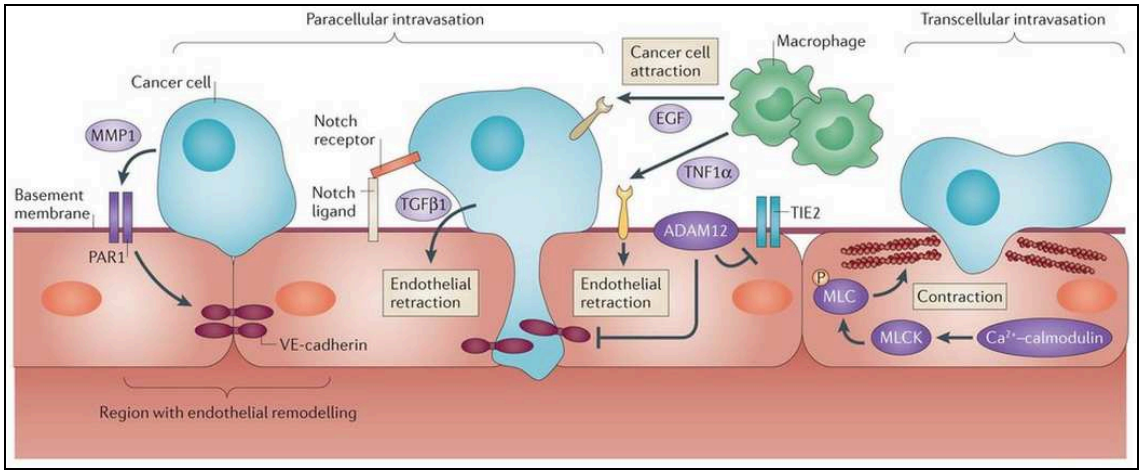

Figure 3- **Schematic view of the modes of intravasation and the underlying cellular and molecular mechanisms** (adapted from Reymon et. al, 2013).

MECHANISMS OF HAEMATIC DIFFUSION

Coping with shear stress

Once in the blood flow, cancer cells are challenged by shear forces dictated by the local shear stress affecting cells either individually (e.g., increasing the extent of cell deformation), or influencing the intermolecular bonds between cells in cases where small clusters of cancer cells are transported through the blood stream. Shear rate governs the rheology of cell transport, modulates the cell-cell collisions taking place between cancer cells, platelets and leukocytes and influences the duration of cell-cell contacts. These interactions affect reciprocally the involved phenotypes. For instance, tumor cells induce platelet aggregation, which then coat tumor cells during their transit through the bloodstream and mediate adherence to vascular endothelium. Platelet-coated tumor cells are protected from shear stresses and the attack from immune cells and modulatory molecules, while stimulated to release an array of bioactive molecules that facilitate tumor cell extravasation and growth at metastatic sites [9].

During extravasation the cancer cell, once opposing the vessel wall, has to contact the endothelial cell and bind to it to be able to arrest and form a stable contact. The first interaction must be established at a relatively low shear rate and depend upon a sufficiently high affinity interaction between “receptor” and “ligand”. Thus, cancer cell adhesion to the vessel wall is the results of a fine balance between cell free velocity, ligand-receptor density, the association and dissociation rates between these molecules, the micromechanical proprieties of each bond and the consequently generated tensile stress.

EGRESSING THE VASCULATURE

The attachment of cancer cells to the endothelial luminal surface is the first step of the extravasation process which typically occurs in small capillaries[10,11]. Cancer cells have been shown to slow down and arrest in capillaries of a similar diameter to that of the cells, which suggests that physical restriction or entrapment of disseminating cancer cells is required for a stable attachment to ensue[10,12]. In the zebrafish model, it has been shown that cancer cells may migrate on the endothelium before extravasating - a phenomenon that may serve the purpose to allow them to

find optimal sites for passing through. As may be expected for the regulation of such a complex process, a wide range of ligands and receptors tightly cooperate to promote extravasation. These include selectins, integrins, cadherins, tetraspanins, integrin-associated moedulatory molecules, CD44 and other cell surface-bound proteoglycans (PGs).

Cancer cells have been shown to roll on the luminal endothelial surface under flow conditions *in vitro*, in a similar way seen for leukocytes, and then initiate more stable attachment[13,14]. However, in contrast to leukocytes, rolling has not yet been described for cancer cells *in vivo*, and indeed it is not observed when cancer cells arrest in capillaries of the liver[12,15] or the brain[10]. However, it is still possible that an initial weak adhesion step could lead to firmer linkage of cancer cells to the endothelium, via engagement of other adhesion mechanisms. Selectins are important receptors in this context, and hence they have been investigated for their involvement in cancer cell adhesion to endothelial cells as well[16,17]. Selectin ligands all include the tetrasaccharide sialyl Lewis x (sLex) antigen, or its isomer sialyl Lewis a (sLea), which can be present on glycoproteins and glycolipids[36].

In humans, increased tumor levels of sLex-modified and sLea-modified glycoproteins generally correlate with poor prognosis. Various glycoprotein ligands for E-selectin are expressed on cancer cells and contribute to the rolling phenomenon seen for various cancer cell lines *in vitro*, including a specific sialofucosylated glycoform of CD44 known as haematopoietic cell E-selectin/L-selectin ligand (HCELL), P-selectin glycoprotein ligand 1 (PSGL1), CD24, mucin 1 (MUC1) and galectin-3-binding protein (LGALS3BP)[18,14,19] (Figure 4). Cancer cell interaction with E-selectin seems to be important for metastasis[20,21], as suggested for colon, breast and prostate carcinoma cells rolling on E-selectin-expressing bone marrow endothelial cells *in vitro* and for the homing of these cells to the bone marrow *in vivo*[22]. E-selectin is not normally expressed on quiescent endothelial cells, but is induced by inflammatory cytokines, which can be secreted by cancer cells themselves or cancer cell-associated leukocytes. This implies that E-selectin may contribute to the cancer cell-endothelium interaction after recruitment and/or activation of macrophages, which then argues against a direct involvement of the selectin in the initial arrest of cancer cells on the endothelium *in vivo*. This also suggests that other receptors, shown to be necessary for the binding of cancer cells to the endothelial surface *in vitro* may more critically be involved in the process *in vivo*.

Among these, CD44 and other PGs are candidate cells surface components contributing to these binding events.

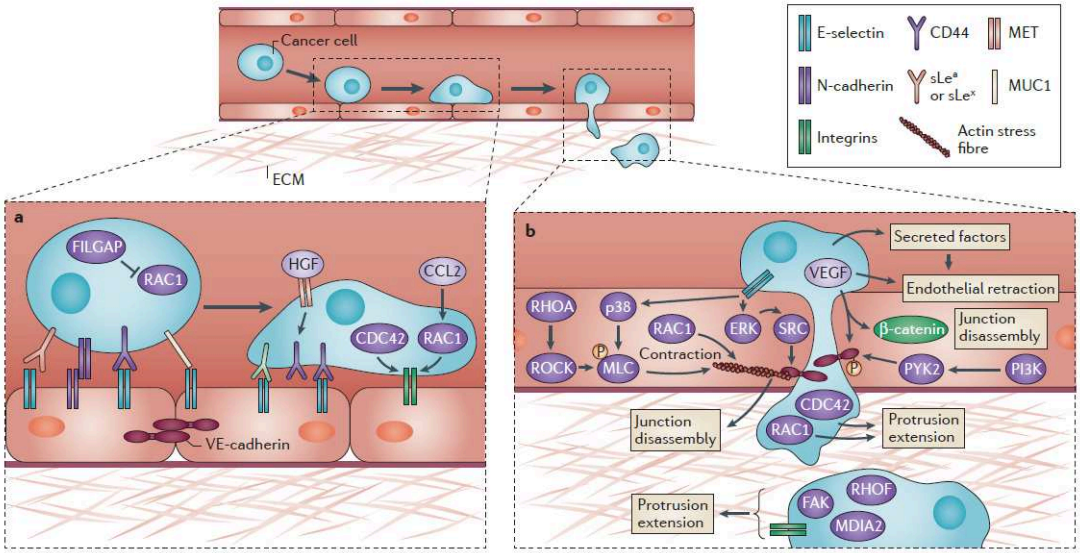

Figure 4- **Adhesion and signaling molecules implicated in cancer cell extravasation. A)** Early attachment of flowing cancer cells to endothelial cells can be mediated by the interaction of endothelial cadherins, selectins, their ligands, CD44 and other PGs, all of which are highly expressed on cancer cells. At this stage, cells maintain a rounded shape, partly because of FILGAP (also known as RHO GTPase-activating protein 24)-induced RAC1 inhibition. HGF increases CD44 expression, whereas cdc42 controls β1 integrin expression and RAC1 stimulates β1 integrin activity. **B)** cdc42 and RAC1 in cancer cells undergoing extravasation drive protrusion extension during transendothelial migration which parallels junction opening induced by secreted factors and/or by engagement of adhesion molecules, such as e.g. the binding of the αVβ3 integrin to PCAM-1. Diffusing cancer cells promote activation of RAC1, RhoA–ROCK and/or p38 MAPK in endothelial cells, which then increase myosin-II phosphorylation, stress fibre formation and actomyosin-mediated tension of endothelial junctions. Disseminating cancer cells can also increase ERK-induced activation of src, and/or activate the PI3-K subunit p110α that functions upstream of PYK2. These pathways are believed to induce phosphorylation (P) and disassembly of the VE-cadherin–β-catenin complex and therefore induce endothelial junction opening. β1 integrins, FAK, RhoF and the diaphanous homologue MDIA2 (also known as DIAPH3) drive the formation of filopodium-like protrusions that are important for the invasion of the basement membrane that surrounds blood vessels and for the subsequent proliferation in the surrounding tissues. CCL2, CC-chemokine ligand 2. (adapted from Reymon et. al, 2013)

In some cases, integrins on disseminating cancer cells also mediate their attachment to circulating blood cells, which then contribute to extravasation. For example, the αVβ3 integrin on melanoma cells was shown to be required for their adhesion to platelets under flow conditions *in vitro*[23,24]. Furthermore, α6β4 integrin was shown to be important for the stable adhesion of colon cancer cells to endothelial cells, after the initial binding of the cancer cells to E-selectin[25]. However, in another study, α2β1 integrin was shown to be upregulated by HGF stimulation in hepatocellular cancer cells, which then led to endothelial cell binding and transvascular movement[26]. Although integrins are clearly involved in cancer cell extravasation, in many cases the relevant α-integrin has not been identified and will

need to be determined to design specific inhibitors of this step of metastasis (Figure 4).

CD44 expression on cancer cells strongly correlates with cancer cell adhesion to endothelial cells and with cancer metastasis[27]. As mentioned above, specific glycosylated forms of CD44 can interact with selectins, and CD44 is required for the adhesion of several cancer cell types to the endothelium and the passage through the vascular wall[28,29]. HGF also upregulates CD44 expression in cancer cells and thereby may increase their adhesion to the endothelium through multiple mediators[29–31]. In addition, CD44 engagement induces signaling that leads to gene expression changes in cancer cells, which then contribute to extravasation. For instance, CD44 crosslinking on breast and colon cancer cells induces the expression of α4β1 and αLβ2 integrins, which have both been implicated in transendothelial movement[32,33].

PROTEOGLYCANS IN THE CONTROL OF TUMOR CELL-VASCULAR BED INTERACTIONS

Proteoglycans (PGs) are macromolecules composed of a central protein structure substituted with covalently attached glycosaminoglycan (GAG) chains. GAGs may be divided in three main families: heparin/heparan sulfate, chondroitin sulfate and its epimerized homolog dermatan sulfate, and keratan sulfate. Inside these families there are different subtypes differing structurally and compositionally and having a diverse tissue localization. All GAGs are characterized by repeating disaccharide units, in particular acetylated hexosamine (N-acetyl-galactosamine or N-acetyl-glucosamine) and uronic acids (D-glucuronic acid or L-iduronic-acid), while keratan sulfate is the only one containing N-acetyl-glucosamine and galactose units. The linkage of GAGs to the core protein involves a specific tetrasaccharide structure composed of two galactose residues and a xylose residue, coupled to the core protein through an O-glycosidic bond to a serine residue (also known as the “linkage region”) except for KS type I where it is linked to the core protein through an N-asparagine bond. GAGs may be modified at various positions by sulfation, epimerization and acetylation. Size and ratio of the GAG chains may change with development, aging or during particular pathological conditions.

The PG family is comprised of certain unique molecules and molecules that share structural similarities with components of other protein families. Conventionally, the classification of PGs is based upon their localization, the type and number of GAG chains attached to the core protein, the size, and the modular composition or the gene.

However, new classifications are now been proposed by our laboratory, entirely on the basis of the PGs' structural characteristics. PGs may function as co-receptors for different ligands, a function that was first believed to be exclusively attributed to their GAG chains. The capacity of GAG chains to differently bind molecules involved in cell-cell and cell-matrix adhesion, cell proliferation and cell motility, appears to be charge-dependent because it is determined by the degree of sulfation of the chain. Another important parameter that influences PG binding capacity is the number and the size of the GAG chains attached to the core protein. Now the PG family includes different molecules that may exist in glycosylated or unglycosylated isoforms, and molecules that are classified as PGs despite being free of GAG chains. It becomes increasingly important to focus also the structural and functional characteristics of the core protein.

PGs are essential components of all tissue of the human body and, as a consequence, they are frequently misregulated in tumors (Table 1). As may be expected of a large protein family, PGs have been implicated in most cellular events and more complex cellular phenomena related to cancer, ranging from cell proliferation to angiogenesis and metastasis formation. Their role in the control of tumor progression is generally multifaceted[32,34–36], but there is still scanty information regarding the involvement of PGs in the processes of intra- and extravasation (Figure 5).

Organ	Tumor type	Proteoglycan[2]
	Glioblastoma	**Agrin, Asporin, Biglycan, Brevican, Fibromodulin, GPC4, NG2, Mimecan, Osteomodulin, PRELP, SDC1**
	Neuroblastoma	**GPC3**
	Head and Neck carcinoma	**Betaglycan, Biglycan, Decorin, Perlecan, SDC1, SDC3, VCAN**
	Laryngeal carcinoma	**Aggrecan, Decorin, SDC1, SDC1^{S}, VCAN**
	Nasopharyngeal carcinoma	**Serglycin**
	Salivary gland adenoma	**Aggrecan**
	Thyroid carcinoma	**Asporin, Biglycan, GPC1, Lumican, NG2, Perlecan, VCAN**

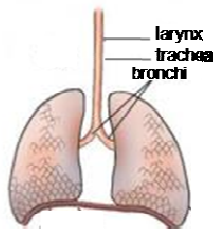	Adenocarcinoma	**GPC3, GPC5, Lumican, VCAN**
	Esophageal carcinoma	**Decorin^{S}**
	Non-small cell lung carcinoma	**Betaglycan, Mimecan, SDC1**
	Small cell lung carcinoma	**Mimecan, SDC1^{S}**
	Squamous cell lung carcinoma	**GPC3, SDC1**
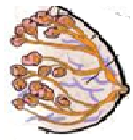	Breast carcinoma	**Asporin, Betaglycan, Decorin, Lumican, GPC1, GPC3^{m}, GPC4, VCAN, SDC1, SDC1^{m}, SDC4^{m}**
	Pancreatic adenocarcinoma	**Asporin, Betaglycan, Biglycan, Decorin, GPC1, Lumican, SDC1, VCAN**
	Cholangiocellular carcinoma	**Agrin, Agrin^{m}, Biglycan**
	Hepatocellular carcinoma	**Agrin, Betaglycan, Decorin, Endocan, GPC2, GPC3, GPC3^{S}, Perlecan, SDC1, VCAN**
	Gastric carcinoma	**Betaglycan, Decorin, GPC3, GPC3^{m}, SDC1, VCAN**
	Renal carcinoma	**Asporin, Betaglycan, GPC1, GPC2, Perlecan**
	Wilms' tumor	**GPC3**
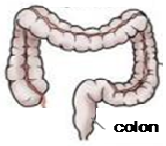	Colorectal carcinoma	**Asporin, Bamacan, Betaglycan, Biglycan, Decorin, Lumican, Mimecan, Perlecan, SDC1, VCAN**
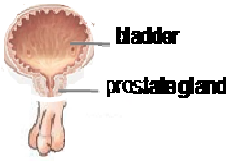	Prostate carcinoma	**Asporin, Betaglycan, Biglycan, Decorin, SDC1, SDC2, VCAN**
	Testicular germ cell tumor	**Decorin, VCAN**
	Urothelial carcinoma	**Asporin, Biglycan, Decorin, VCAN**
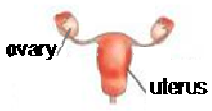	Cervical/endometrial carcinoma	**Asporin, Biglycan, Decorin, Lumican, Perlecan, SDC1, SDC3, SDC4, VCAN, VCAN^{m}**
	Ovarian carcinoma	**Asporin, GPC3, VCAN**
	Ovary clear cell carcinoma	**GPC3**

	Melanoma	**Asporin, Perlecan, VCAN, NG2, GPC3, GPC3^{S}**
	Fibrosarcoma	**NG2**
	Chondrosarcoma	**Aggrecan**
	Leiomyosarcoma	**Decorin, NG2**
	Liposarcoma	**Decorin, Decorin^{m}, NG2**
	Neurofibrosarcoma	**Decorin, Decorin^{m}**
	Pleomorphic sarcoma	**Biglycan, Decorin, Decorin^{m}, NG2**
	Rhabdomyosarcoma	**Decorin ,GPC3, GPC5**
	Synovial sarcoma	**Decorin**
	Myeloma	**SDC1, SDC1^{S}**
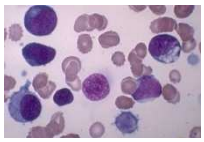	ALL(-B/-T)	**NG2**
	AML	**Serglycin**
	CLL-B	**Fibromodulin, SDC1**
	Hodgkin's lymphoma	**SDC1**
	Mantle cell lymphoma	**Fibromodulin**
	Non-Hodgkin's lymphoma	**SDC1**
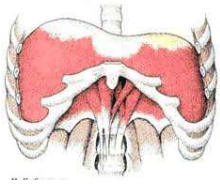	Mesothelioma	**GPC3, SDC2**

Table 1- ***Distribution pattern of PGs in cancer*** .Data refer to PG expression at either mRNA and/or protein level in the indicated tumors when compared to healthy counterpart tissues or benign forms. "^{S}"refers to PGs detected in blood; "^{m}"refers to assessment of PG expression at either mRNA and/or protein level in metastatic *versus* primary lesions; [2]*red*, hyaluronan-binding PGs; *green*, collagen-associated PGs; *purple*, basement membrane PGs; *blu*, cell-surface PGs; *orange*, Intracellular PG. *Abbreviations*: GPC1-5, Glypican-1-5; SDC1-4, Syndecan-1-4; VCAN, Versican. Modified from Garusi et al., 2011.

The abundant expression of multiple cell surface PGs and the complex patterns of ECM PG synthesis and secretion by neoplastic cells imply a direct involvement of these macromolecules in the control of the tissue interactions sustaining tumor growth and dissemination. In fact, PGs are recognized as being implicated in the two principle cellular events conducive to metastasis formation: cell motility and tissue invasion (Figure 5). To contribute to these cellular phenomena, cell surface-associated PGs may either directly link to the ECM or modulate the activity of integrins [37] and other matrix receptors.

Overall, cell surface PGs may either act as promoters of tissue invasion and metastasis formation, as demonstrated for syndecan-1, GPC1 and NG2/CSPG4 (*see below*). In the case of syndecans, alternative promoting or inhibiting functions may depend upon their differential ability to serve as co-receptors with ligand specificities dictated by their GAG chain diversity[38,39]. This idea has its grounds in the fact that syndecan-1 has been reported to induce intracellular signal transduction independently of integrins[40] and that binding of a variety of tumor cell types to laminins requires a syndecan-1-substrate interaction[41–44]. A similar putative interaction of syndecan-1 with ECM components involves thrombospondin-1[45]. More recently, it has became clear that syndecan-1 operates as an immediate regulator of the activity of αvβ3, αvβ5 and α6β4 on breast carcinoma cells[46,47], presumably through a linkage of its cytoplasmic tail with the intracellular portion of integrins[48,49].

It has further been suggested that syndecan-1, -2 and -4 act in concert with multiple integrins (e.g. α2β1, α5β1, α6β1 and αv-containing integrins) in different tumor cell lines to specifically affect the cells' fibronectin-, vitronectin-, collagen- and laminin-binding. These syndecans have also been suggested to influence tumor cell invasion through collagenous fibrillar matrices, in part by intervening in lamellopodia formation through Tiam-1 and Rac1 activation[50–52]. However, it remains to be ascertained whether cooperation of syndecans with integrins affects cell adhesion and migration in a positive or negative fashion[43,52–55]. It would be equally crucial in this context to determine the precise syndecan-Rho-lamellopodia-filopodia interplay relationship[36,56–62]

NG2 also serves as a mediator of membrane-ECM interactions taking place in moving cells and may also be critical in establishing a continuum between the microenvironment and the actin cytoskeleton (Figure 5).

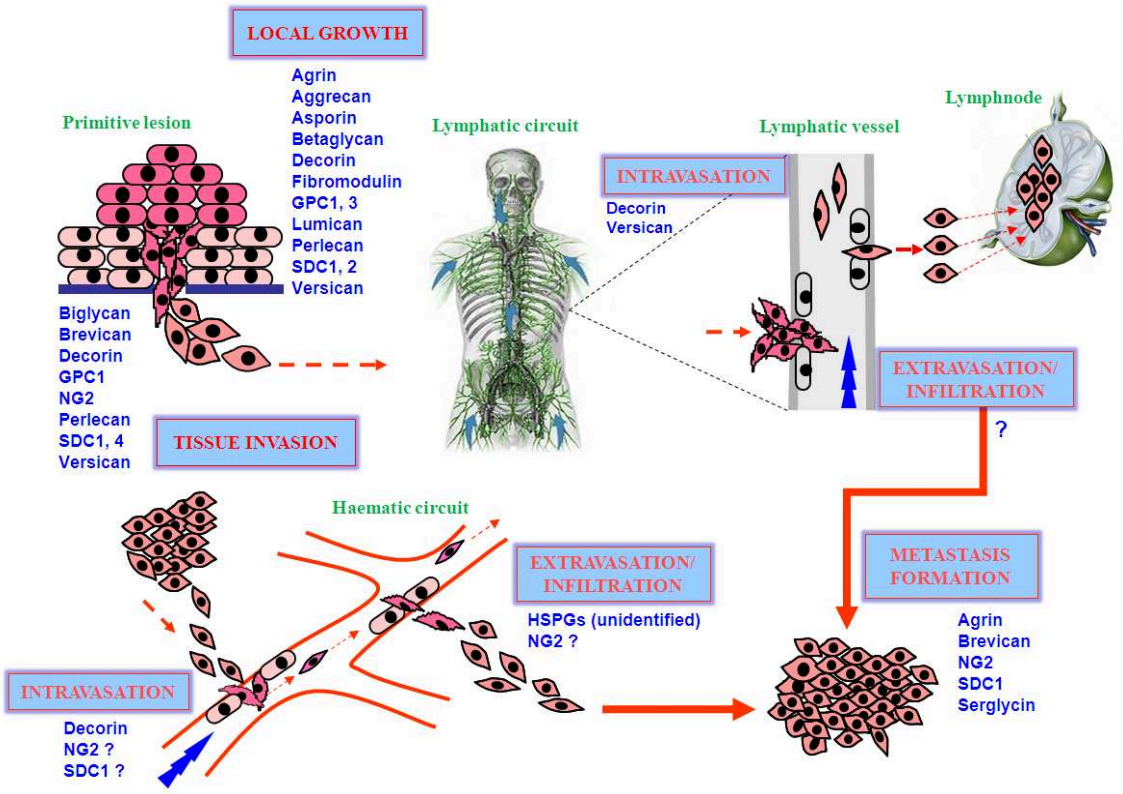

Figure 5- ***Schematic overview of the putative PG involvement in the different phases of tumorigenesis.*** A number of PGs expressed by the tumor cells themselves or by the intralesional stroma promote *local growth* (an may also affect intra-lesional angiogenesis). By contrast, very little is known about to what extent PGs may contribute to local tissue invasion, the entrance (*intravasation*) of disseminating cells into the haematic and lymphatic circuits, and their exit from these circuits in target organs (*extravasation*). HS-bearing PGs have been proposed to be implicated in the process of leukocyte/lymphocyte extravasation (which is thought to be regulated by mechanisms analogous to those governing tumor cell trafficking), but the identity of these PGs has not yet been disclosed. Cell surface PGs, in their membrane-associated or shed form, are similarly believed to the implicated in this phenomenon and our preliminary findings assigns a pivotal role to NG2 in this process and the recycling disseminating cancer cells through the circulation. A number of PGs have also been demonstrated to be associated with *metastasis formation* in various experimental models and most of these PG are accordingly found to be up-regulated in human metastatic lesions (adapted from Garusi et al., 2011).

NG2/CSPG4 IS A PRIMARY MEDIATOR OF THE CANCER CELL'S INTERACTIONS WITH THE MICROENVIRONMENT

NG2/CSPG4 is a unique transmembrane PG (Figure 6) that may be accounted for many of the interactions taking place between tumor cells and their microenvironment during both cell propagation and cell movement[63,64]. It was coincidently identified on melanoma cells[65,66,67], where it was found to be part of a repertoire of antigens characteristic of these neoplastic cells and, because of its large

size, was named High Molecular Weight Melanoma-Associated Antigen [HMW-MAA or simply Melanoma-associated Chondroitin Sulfate Proteoglycan - MCSP], and in the rat central nervous system where it appeared to be implicated in neuron-glial interactions and was assigned the name NG2 (Neuron-Glia Protein 2) [68].

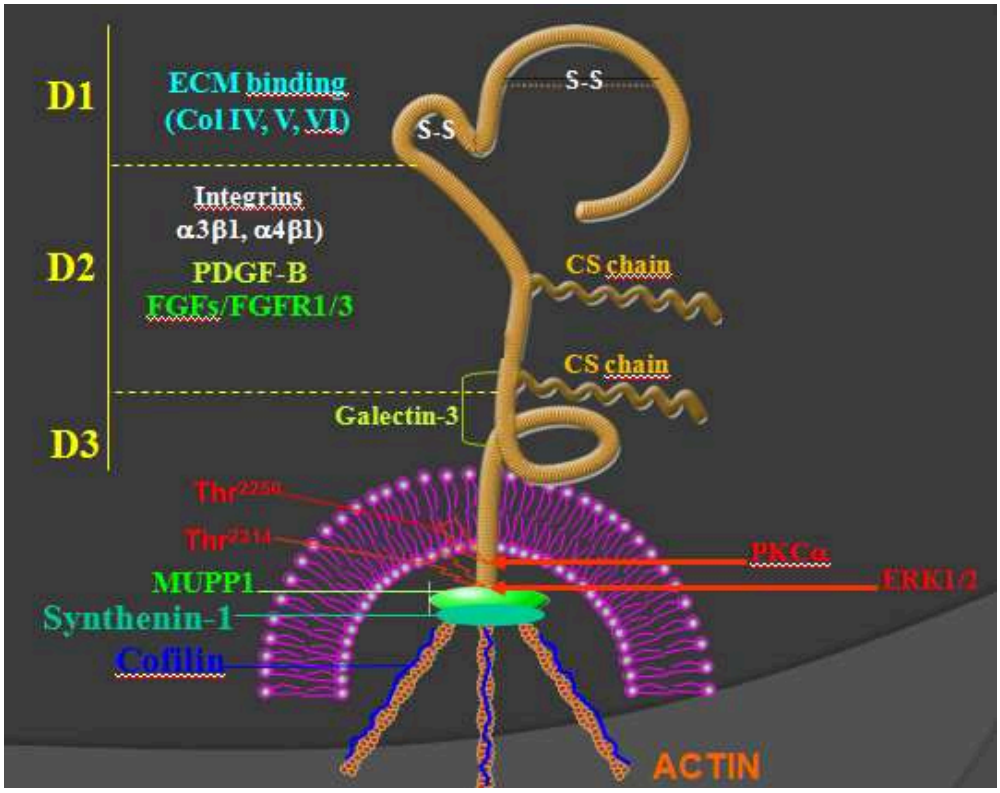

Figure 6: **Schematic rappresentation NG2/CSPG4 different domains**

In the adult human body, NG2/CSPG4 has a limited tissue distribution and is characteristically found with prevalence on immature and progenitor cells of various tissues and organs, including brain, skeletal muscle, cartilage and skin (Human Proteome Resource Project, www.proteinatlas.org; own data). It is generally absent from all mature epithelial and hematopoietic cells, while it becomes de novo expressed upon neoplastic transformation of different cell types with the most striking examples being its appearance on melanocytes converting into melanoma and T lymphocytes and myeloid cells turning into leukemic cells[67,69].

Cloning of the NG2/CSPG4 gene, originally accomplished in rat[68], and much later on in man[70], revealed that the gene is localized on the human chromosome 15:24q2[71], encodes for a 8.9 kb transcript with an open reading frame of 8,071 nucleotides which translates into a core protein of 2,325 residues encompassing numerous

glycosylation sites and three putative glycosaminoglycan (GAG)-attachment sites. In its fully glycosylated form NG2 has an apparent molecular size of >500 kDa[72,73] and detailed ultrastructural and sequences analyses of the NG2/CSPG4 ectodomain can be subdivided three distinct subdomains: a globular N-terminal, D3, a flexible rod-like central segment, D2, and a C-terminal one, D1, assuming an extended globular conformation (Figure 6). The D3 subdomain contains 4 phylogenetically conserved Ca^{2+}-binding cadherin-type repeats, whereas the membrane proximal one encompasses at least two distinct proteolytic cleavage sites attacked by metalloproteinases in part antagonized by TIMP2 and TIMP3. These contribute to both the physiological and disease-associated shedding of the ectodomain from the cell surface by a cell-autonomous signal transduction-dependent mechanism and producing at least two tryptic forms of the PG having apparent MW of 290 kDa and 275 kDa.

The cytoplasmic tail of NG2, stretching 76 amino acids, contains two threonine residues prone to differential phosphorylation by PCKα (Thr^{2256}) and ERK1 (Thr^{2314}), depending upon whether the PG engages in migration or proliferation events[74,75]. Through the cytoplasmic tail NG2/CSPG4 firmly links to the actin cytoskeleton via bridging of PDZ-type adaptor proteins such MUPP1 and synthenin-1[72,74,76] and close association with ezrin and cofilin-1 (Figure 6). Through cytoskeletal connections and the above mentioned PCKα/ERK-dependent threonine phosphorylations, the intracellular domain of NG2/CSPG4 also activates signalling cascades involving FAK, Rac1, cdc42, Ack1 and p130[CAS 64,74,77] , suggesting that that it may contribute to the execution of intricate patterns of signal transduction governing cytoskeletal dynamics.

A solid trait of NG2/CSPG4 remains the continuum that it creates between the extracellular environment and the inside of the cell through its connection with actin microfilaments both distinct at filopodial tips (microspikes) and at the level of the lamellipodia and retraction fibres of highly motile cells (Figure 6). The primary ECM ligand of NG2/CSPG4 is collagen type VI (Col VI)[78,79,75] and, although some studies have suggested that it may also bind to collagen types II, IV and V, vitronectin and tenascin-C, the NG2-Col VI interaction appears as a crucial factor in the control of tumor growth and spread[76,64]. A more direct effect of NG2/CSPG4 on cell adhesion spreading and motility has been proposed to be exerted on both sprouting pericytes and tumor cells, through modulation of the function of integrin

α3β1 and α4β1 with which NG2/CSPG4 may associate on the cell surface[75,79,76]. The presence of NG2/CSPG4 on the cell surface strongly impacts on the growth of the cells and this ability is provided through a well-described docking receptor function of the PG in cells responding to PDGF-AA[34]. A recent investigation demonstrates that NG2/CSPG4 also plays a crucial role in the control of the mitogenic responses to various members of the FGF family[80,17]. In fact, in NG2/CSPG4 null mice, FGF-elicited corneal angiogenesis is strongly impaired due to a failure of pericytes to undergo normal extension and propagation[70,81]. Detailed analysis of FGF signalling dynamics in isolated NG2/CSPG4-expressing and NG2/CSPG4-deficient cells indicates that the PG governs both paracrine and autocrine FGFR1-mediated mitogenic responses, in part docked by FGFR3. Taken together the growth factor co-receptor function of NG2/CSPG4 and its potential ability of sequestering angiostatin may explain the pivotal support of NG2/CSPG4 pericyte sprouting and tubular formation.

There is evidence that in soft-tissue sarcomas, enhanced expression of NG2/CSPG4 provides the first, independent molecular marker of prognosis and uniquely predicts with a >55% probability formation of lung metastases within 12 months post-surgery. Finally, clinical trials on advanced melanoma patients in which NG2/CSPG4 has been targeted immune-therapeutically, either directly or through anti-idiotypic antibodies have yielding strikingly positive results. Cumulatively, these findings corroborate a central role of NG2/CSPG4 in tumor progression and emphasize the potential of the PG as a therapeutic target.

AIMS OF THE STUDY

Experimental data has thoroughly suggest that vascular cells, including pericytes, and their associated ECM are key players in the control of transvascular passage of tumor cells and a plephora of cell surface components expressed by these cell types are believed to act as mediators. Cell surface proteoglycans (PGs) are among the components believed to play an active role in this context, although it is not known how, and in particular NG2/CSPG4 seems to be a good candidate regulator of the cellular interactions ensuing during extravasation. This study focuses on the potential of role of NG2/CSPG4 in mediating the interaction of cancer cells with the endothelial surface and with the perivascular ECM. To this end the study has made

use of experimental paradigms of cell adhesion, migration and invasion, under static and dynamic, shear rate-dependent assays. In parallel, a protocol was re-adapted for the in vitro isolation of native, cell-free perivascular matrices for their structural-functional characterization and for testing on cells. Sarcoma and melanoma cell subsets immunosorted for their expression of NG2/CSPG4 were used as model tumor cells for addressing the ability of NG2/CSPG4 to mediate interaction of disseminating cancer cells with the vascular bed and its associated ECM. In this context, CAM assays are utilized to explore the function of the PG in intra- and extravasation settings in vivo, whereas global gene and phospho-proteomic profiling were used to define whether enhanced expression of NG2/CSPG4 was associated with gene expression patterns characteristic of malignant cells harboring altered signal transduction pathways. The findings of the study contribute to our understanding of the pro-metastatic role of NG2/CSPG4 seen in animal models and support the consistently observed, enhanced expression of the PG in metastatic lesions of different tumor types. Starting from these observations, it may be envisioned that NG2/CSPG4 may favor metastasis formation by governing specific steps of the metastatic cascade and, hence, may be considered as a valid target for anti-metastatic therapeutic approaches.

RESULTS

NG2/CSPG4 EXPRESSION DOES NOT CORRELATE WITH MIGRATION POTENTIAL

There is ample experimental evidence that enhanced levels of cell surface NG2/CSPG4 conferred to cells a better capability to interact with their microenvironment[43], thereby affecting the growth and spreading capabilities of tumour cells. To establish a more precise connection between high levels of the PG and the ability of cancer cells to exhibit a more aggressive phenotype, we first determined the relative cell surface levels of the PG in a larger number of model cell lines (Table 2).

Cell lines	Tumor type	Percentage of positivity to NG2
143B	osteosarcoma	100 (20 weakly)
MG63	osteosarcoma	96
Saos2	osteosarcoma	100
SKLMS1	leiomyosarcoma	95 (25 weakly)
DMR 94278	leiomyosarcoma	100
SKUT1	leiomyosarcoma	100 (30 weakly)
HT1080	fibrosarcoma	100
Hs913t	fibrosarcoma	100 (5 weakly)
GCT	fibrous histiocytoma	1000
97441b	fibrous histiocytoma	100 (15 weakly)
SW 872	liposarcoma	100 (30 weakly)
RD/KD	Rhabdomyosarcoma	100 (5 weakly)
A204	Rhabdomyosarcoma	100 (5 weakly)
MESSA	sarcoma uterin	100 (15 weakly)
U87	neuron glial	100
U251	neuron glial	100 (very weakly)
Mewo	Melanoma	30
Memor	Melanoma	60
Memi	Melanoma	0
Mecop	Melanoma	100
M2	Melanoma	100
A375	Melanoma	100
C32	Melanoma	100
M14	Melanoma	0
Meta	Melanoma	100
Mepa	Melanoma	100
Meov	Melanoma	100
mefo1	Melanoma	100

Table 2**- Flow cytometric analysis of NG2/CSPG4 expression in model cancer cell lines** based upon immune-detection with anti-NG2/CSPG4 mAb 7.1 PE-conjugate, in some cases followed up by confirmatory immunoblotting.

Consistent with previous findings, the majority of the sarcoma and melanoma cell lines that were assayed exhibited significant surface levels of the PG and further immunochemical analyses with a number of propriety antibodies confirmed this expression pattern. Particularly widespread was the frequency of NG2/CSPG4 expression of these tumor cells, with most types having virtually all cells of the population expressing the PG, albeit, in some cases, at lower levels.

The panel of model cell lines for which we defined the relative surface levels of NG2/CSPG4 were assayed for their migratory abilities in conventional scratch assays. Somewhat unexpectedly, in this setting, cells with high levels of CSPG4/NG2 moved less effectively that cells with lower levels of the PG and, overall, there was no clear relationship between motility rates and surface levels of NG2/CSPG4 .Figure 7).

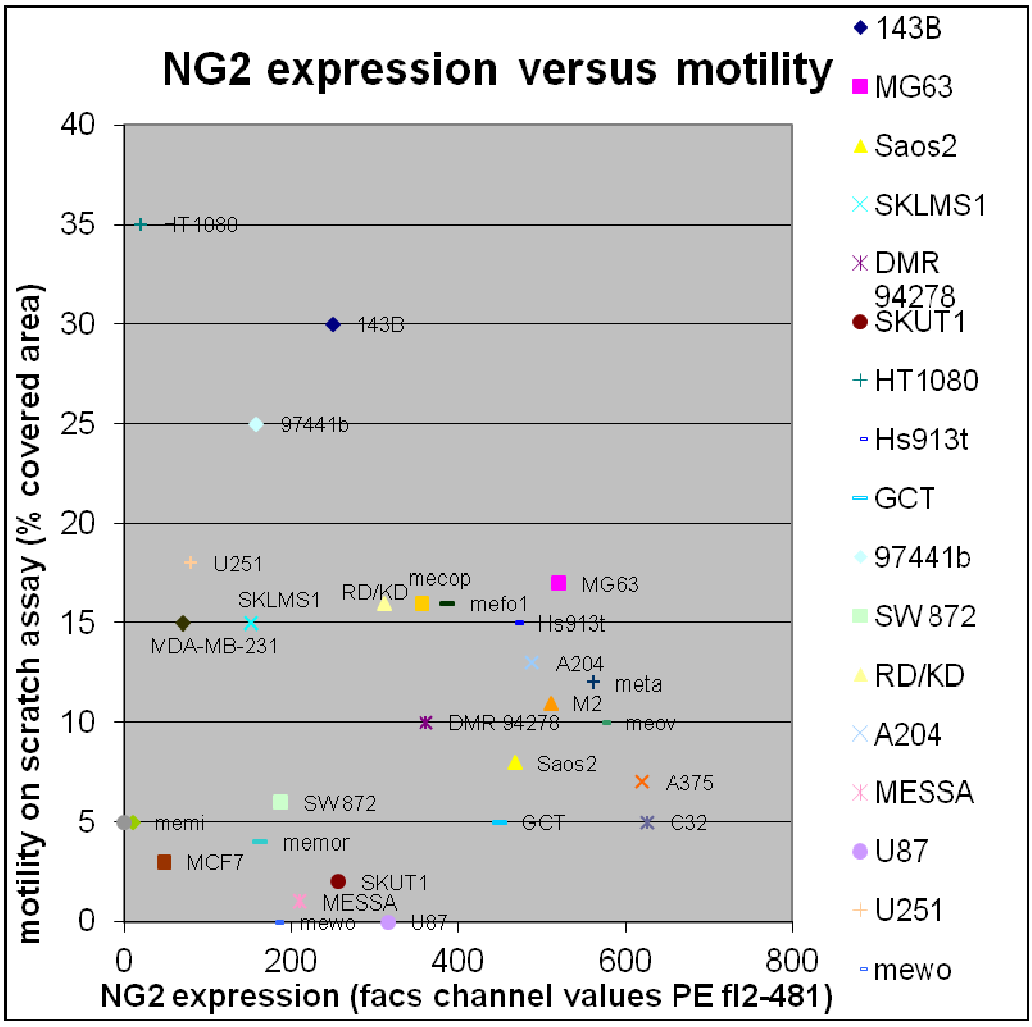

.Figure 7: **Relationship between constitutive NG2/CSPG4 expression and migratory capability of the panel of sarcoma and melanoma cell lines** when compared to that of two highly motile breast carcinoma cell lines, MDA-MB-231 and MC7.

When examining NG2/CSPG4 expression levels in different cell lines, we noticed that in some of them its distribution within the cell population was heterogeneous (Table 2) suggesting that NG2/CSPG4 expression was proper of specific subsets of cells. Such pattern was largely consistent with the distribution of the PG previously observed in soft-tissue sarcoma, breast carcinoma and melanoma lesions and largely paralleled that reported from other tumor types. We then explored the possibility to separate the NG2/CSPG4-expressing cell subset by means of immunosorting such as to create model cell lines with diverse constitutive levels of the PG. To this end we compared the efficacy of immunomagnetic and FACS approaches *(see Material and Methods)*, based upon the well-established anti-NG2/CSPG4 monoclonal antibody 7.1. We also exploited the use of a propriety anti-NG2/CSPG4 monoclonal antibody which yielded analogous sorting efficiencies. Fluorescence-based sorting methods were noted to superior to immunomagnetic approaches, especially in cases in which the NG2/CSPG4-expressing subset represented a markedly smaller subpopulation. A FACS method was therefore preferred and was applied to a variety of cell lines in which the NG2/CSPG4-expressing cell population was ≥5% of the entire population (i.e. in cases of subpopulations that were more rare we were not able to effectively separate homogeneous subsets).

Evaluation of a larger panel of cell lines in which we immunosorted the NG2/CSPG4-expressing subsets revealed three different scenarios: 1) immunosorted cells failed to maintain the phenotype and either silenced the expression of NG2/CSPG4 in the PG-positive subset, or re-expressed NG2/CSPG4 in the PG-negative subset; 2) separation of the two cell subsets yielded one subpopulation that failed to propagate and 3) cell lines in which the two immunosorted subpopulations were equally effective in propagating and could be established by flow cytometry to be more than 80% pure phenotype (Table 3). This latter situation assured us to be able to adopt the immunosorted NG2/CSPG4-expressing subsets as model cells for further in vitro and in vivo analyses.

Cell type	%NG2	cell sub-population	% NG2 at sorting	% NG2 after more passages or resorting
HT1080	5	NG2+	95	
		NG2-	5	
MESSA	75	NG2+	93	(p18) 70
	15%weakly	NG2-	83	(p18) 64
SKLMS1	95	NG2+	95	
	5 weakly	NG2-	73	
MEWO	70	NG2+	87	
		NG2-	0	
MEMOR	60	NG2+	100	resorting: 35% after 2 passages
		NG2-	60	
MDA231	70	NG2+	80	
		NG2-	60	
143B	80	NG2+	97	
	20 weakly	NG2-	78	

Table 3- **Characteristics of immunosorted NG2/CSPG4-expressing cell subsets**.Immunosorted cell lines were obtained separating cells belonging to the same cell population according to the expression of NG2/CSPG4 using the patented MACS® columns and beads conjugated (Myltenyi Biotec GmbH, Germ)

In this way we were able to test the cell behaviors in various conditions using two tumor model that present very different characteristics: body districts colonization, type of injury, way of growth, etcetera. At the same time we were able o study and evaluate the influence played by NG2/CSPG4 presence on cell surface on tumor development in a contest non tumor specifically linked. In other words we were able to evaluate if the effect generated by the presence or the absence of NG2/CSPG4 was a dependent from the specific type of tumor, or if it takes place in an independent way. That was the force of our study.

NG2/CSPG4 PROMOTES TUMOUR GROWTH *IN VIVO* MODEL

Previous studies have demonstrated that tumour cells presenting NG2/CSPG4 exhibit a more aggressive phenotype. To verify this notion, we designed xenografting experiments entailing sarcoma and melanoma cell subsets with different constitutive levels of expression of NG2/CSPG4. For this purpose we separated by immunosorting of CSPG4/NG2$^+$ and CSPG4/NG2$^-$ subpopulations of a number of sarcoma, melanoma and breast carcinoma cell lines (*see Material and Methods*) and compared their tumorigenic potential in vitro and by transplantation into nude mice.

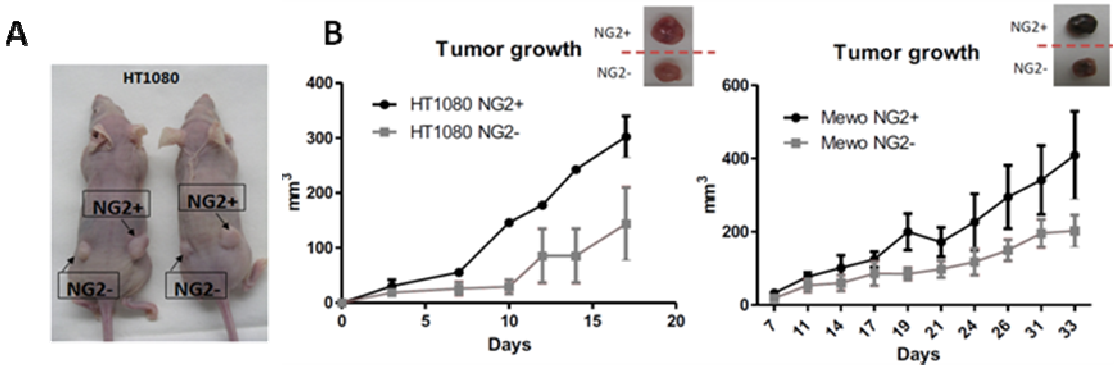

Figure 8 - **Representative growth kinetics of NG2/CSPG4 expressing and non-expressing cells in vivo**: A) subcutaneous implantation into nude mice of the HT1080 NG2$^-$ and NG2$^+$ cells; B) locally growing tumors induced by subcutaneous implantation into nude mice of HT1080 NG2$^+$ and NG2$^-$ or MeWo NG2$^+$ and NG2$^-$ cell subsets.

Both unilateral and paired bilateral flank transplantations (i.e. each of the cell subsets was implanted on either flank of the same animal) were performed. These experiments showed that the CSPG4/NG2+ cell subsets developed conspicuous tumours after a short time period, whereas, within the same time period, the CSPG4/NG2- cell formed smaller masses. Starting from this observation, we decided to set up different *in vitro* assays in order to better investigate the NG2/CSPG4-dependent cell behaviour.

CSPG4/NG2 PROMOTES CELL SURVIVAL UNDER STRESS CONDITIONS, BUT DOES NOT MODIFY PROLIFERATION RATES UNDER OPTIMAL GROWTH CONDITIONS

Previous studies of the laboratory and other investigators have provided hints about the possibility that tumor cells expressing high levels of CSPG4/NG2 may be more resistant to stress conditions, though the underlying mechanism has not been disclosed. To approach this problem we verified the capability of sarcoma and melanoma cells to survive under stress conditions. For this purpose we initially cultivated NG2/CSPG4-expressing and non-expressing cells in the absence of serum and evaluated their overall survival rates. The presence of NG2/CSPG4 on cell surface seemed to confer a higher resistance to nutrient deprivation (Figure 9)

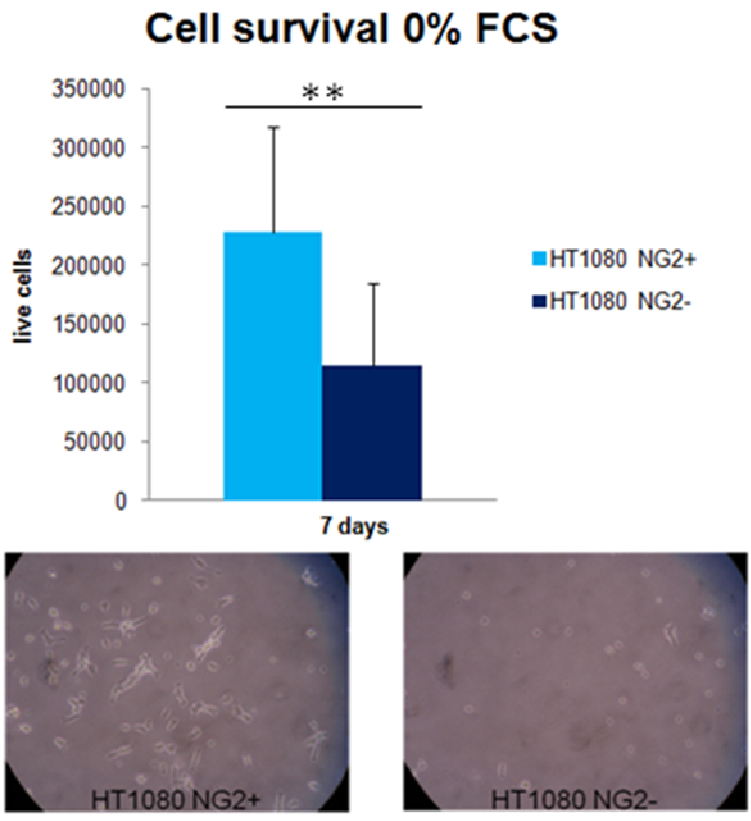

Figure 9- **Degree of NG2/CSPG4-dependent cell survival under nutrient deprivation** (*:p<0.5; **:p<0.05; ***:p<0.005).

We next used BrdU incorporation to examine whether the proliferation potential of NG2/CSPG4-expressing and non-expressing cell subsets differed in

conditions of exponential growth. No significant differences were observed when HT1080 NG2+ were compared to HT1080 NG2- cells (Figure 10). Similar results were obtained when MeWo NG2-expressing and non-expressing cells were compared with each other (data not shown).

The observed enhanced survival rates of NG2/CSPG4-expressing cells suggested that these cells could be advantaged in a situation of anchorage-independent growth. We therefore tested this possibility in immunosorted melanoma and sarcoma cells: morphological transformation of cell colonies induced by chemicals is associated with certain phenotypic changes such as loss of contact

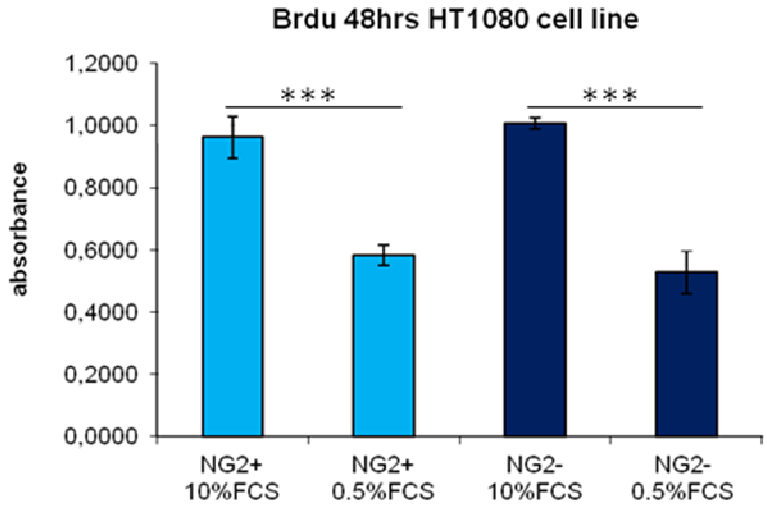

Figure 10 – BrdU incorporation in NG2/CSPG4+ and NG2/CSPG4- **HT1080 cells.** Cells were starvated for 48h with 0.5% FCS medium, the same cell subpopulation grown in complete medium were used as positive control. Starvation slows down DNA synthesis both in HT1080 NG2 + and HT1080NG2- cells. . (*:p<0.5; **:p<0.05; ***:p<0.005).

inhibition (cells can grow over one another) and anchorage independence (cells form colonies in soft agar). Anchorage independence can be described in the light of primary fibroblasts and many fibroblastic cell lines (e.g. BALB/c3T3, NIH-3T3, etc.) that must attach to a solid surface before they can divide. They fail to grow when suspended in a viscous fluid or gel (e.g. agar or agar), however when these cell lines are transformed, they are able to grow in a viscous fluid or gel and become anchorage-independent. The process by which these phenotypic changes occur, is assumed to be closely related to the process of in vivo carcinogenesis. These systems are believed to be reasonably good predictors of in vivo activity, and positive results are viewed as potential indications of in vivo carcinogenesis: tumor cell proliferative potential increases with increasing aggressiveness.

To prepare this test we plated 2500 cells for each well using a 6 well Petri plastic dish and we improved 5 experiment each cell line. We tested the melanoma and the sarcoma immunosorted cell lines. So we analyzed MeWo NG2+ , MeWo NG2-and HT1080 NG2+ and HT1080 NG2- cells using the same experimental condition.

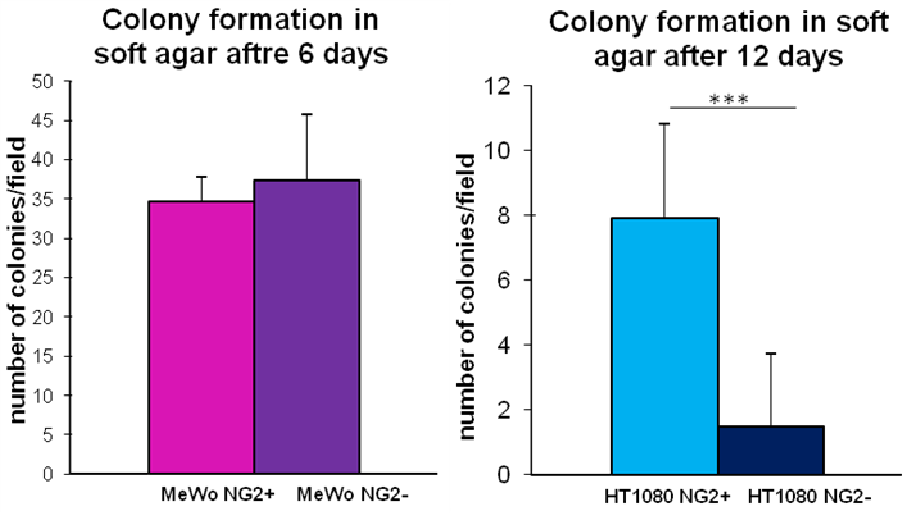

Figura 11- **Soft agar assay:** 2500 cells suspended in complete medium recostituited agar and plated in each well using a 6 well Petri plastic dish, 5 experiment each cell line improved. The colony count was made at different times after plating depend by cell line types. (*:p<0.5; **:p<0.05; ***:p<0.005).

No differences were noticed between the MeWo two subpopulations nor in a week (as we reported on histogram in Figura 11) neither a 12days after plating. Very interesting was the behavior of sarcoma subpopulation cells: HT1080 NG2+ cells were more able than the negative ones to form colonies and the biggest differences were observed after 12 days plating. Thanks to this data we confirmed again that the presence of NG2/CSPG4 proteoglycan on cell surface in some tumor type correlates with a most aggressive phenotype.

In a parallel approach flow cytometry using fluorescent Annexin-V was used to evaluate the relative frequency of apoptotic cells. It is well known that cells that grow in adhesion when achieve the confluence state start to die off and may not be recoverable. It is easy to imagine that confluence is an important stress source. To assess the relationship between the presence of NG2/CSPG4 on cell surface and the resistance to confluence state, we chose HT1080 cell lines for the same reasons explained before and we set up an experimental protocol by growing the cells until the confluence and monitoring them for 4 days. After this period the cells were

detached from the plastic plate and assayed by citofluorometry for Annexin V. The subpopulation expressing NG2/CSPG4 as a membrane proteoglycan shows a lower rate of mortality under over-confluence stress condition than the NG2/CSPG4 negative subpopulation, so it seems to be more stress resistant that the other one (Figure 12). In fact, comparing the data obtained from this assay, the number of HT1080 NG2+ dead cells was four time less than the HT1080 NG2- ones.

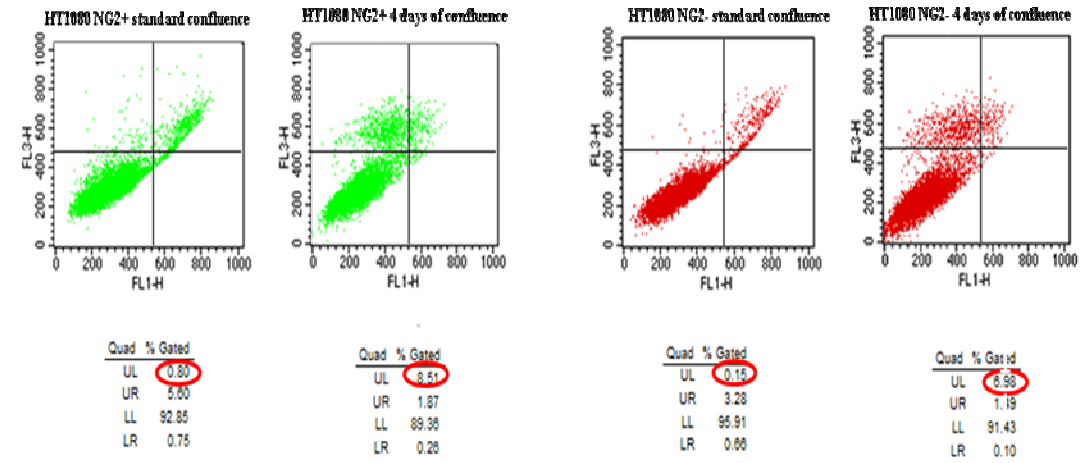

Figure 12 – Apoptotic rates of NG2/CSPG4 expressing and non-expressing cells as determined by **FITC-Annexin V flow cytometry**. Levels of Annexin V-binding were evaluated in HT1080 NG2+ and HT1080 NG2- cells after 4 days of starvation. The red rings indicate the quantity of alive cells before and after starvation. From the relationship between this values it is possible to estimate how strong was the effect of starvation on cell survival.

ROLE OF NG2/CSPG4 IN THE CONTROL OF CELL MOTILITY AND INVASION

To establish the putative role of NG2/CSPG4 in the control of cell migration and invasion, we performed a matrigel evasion test: this assay permits to estimate both cell motility and cell response to chemoattractant. In particular we assayed the differential capability of NG2/CSPG4-expressing HT1080 cells to migrate through a compact ECM in the presence or absence of serum. Cells were included in a 6 mg/ml matrigel solution in presence of different concentration of FCS. Cell drops were plated on plastic multiwell plates and after the matrigel polymerization, complete medium 10% serum was added all around the drops: it functions as chemoattractant. Cells that are in a poor medium try to move to reach the complete medium.

The subpopulation of sarcoma cell line HT1080 were tested in a very strong condition of 0.5 % of serum on drop to try to stimulate them to move known their capability to resist in bad conditions. On the other side, the two melanoma subpopulations that appear less resistant under stress condition, were tested 5% FCS matrigel drops. Four days after inclusion we estimated the evasion ability using a phase-contrast microscope and we noticed that both in sarcoma and in melanoma cells the NG2 positive subpopulation migrated less than the NG2 negative one, in accord to the observation that when the proteoglycan is present, cells are more able to take in contact with the microenvironment so they move less (Figure 13).

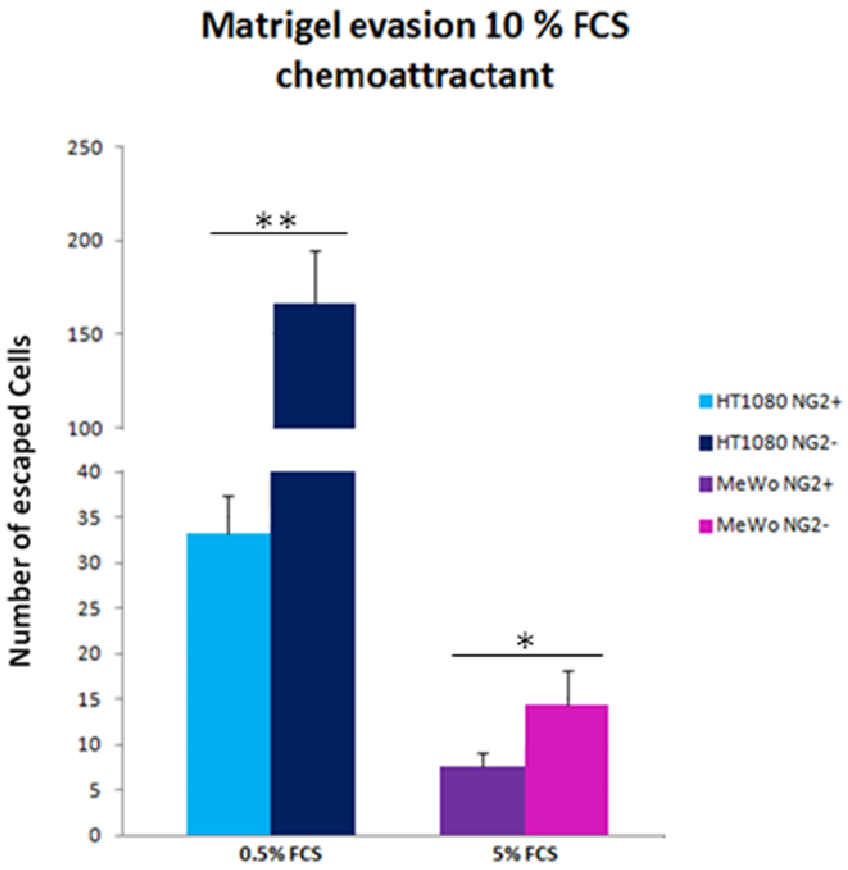

Figure 13- **Evasion assay** set up generating a FCS gradient between the inside matrigel drop (poor for FCS concentration) and the outside matrigel drop (enriched for FCS concentration). There were tested sarcoma and melanoma subpopulations immunosorted for the presence of CPG4/NG2. (*:p<0.5; **:p<0.05; ***:p<0.005).

Cell capability to move was tested by scratch assays too. In this assay cells were grown until confluence. Eight hour before starting the test cells were starved with 0,5% FCS medium, than the monolayer was then scratch with a tip and cells were maintained on starvation in order to inhibit cell proliferation and to could test the cell real ability to move. In the next 24 hours cells could migrate in order to cover the area cell free created by the scratch. To do this experiment we use HT1080 subpopulation because their capability to move quickly. After 24 hours in fact the injury was completely repair by the HT1080 NG2+ subpopulation but it was repair just in part by the HT1080 NG2- one (Figure 14).

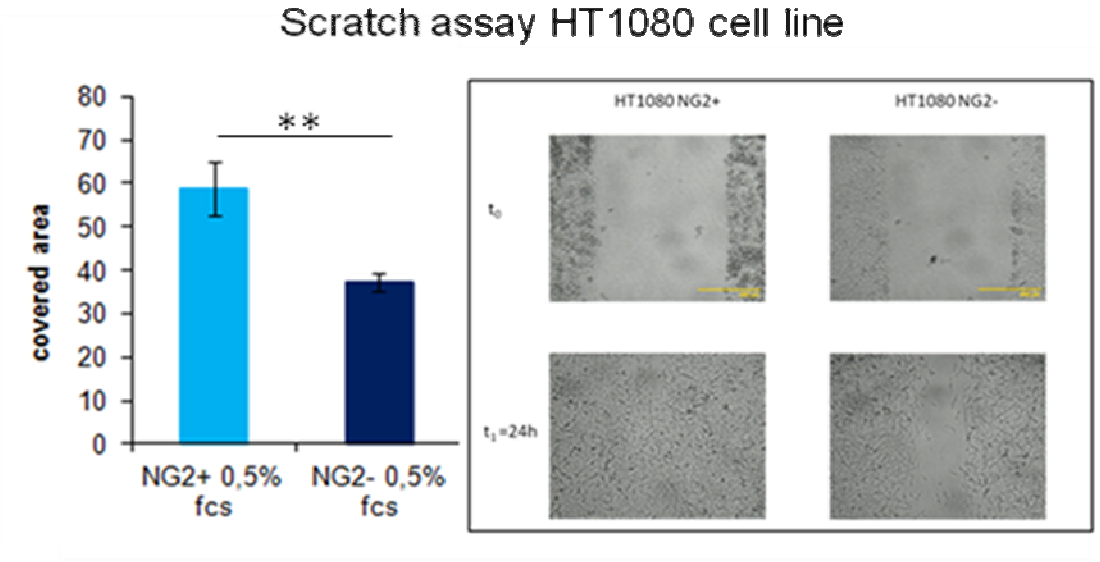

Figure 14- **Motility assay**: HT1080 NG2+ and HT1080 NG2- cells were tested by scratch assay. . (*:p<0.5; **:p<0.05; ***:p<0.005).

GENE MODULATION IN CELLS EXPRESSING DIFFERENT LEVEL OF NG2/CSPG4

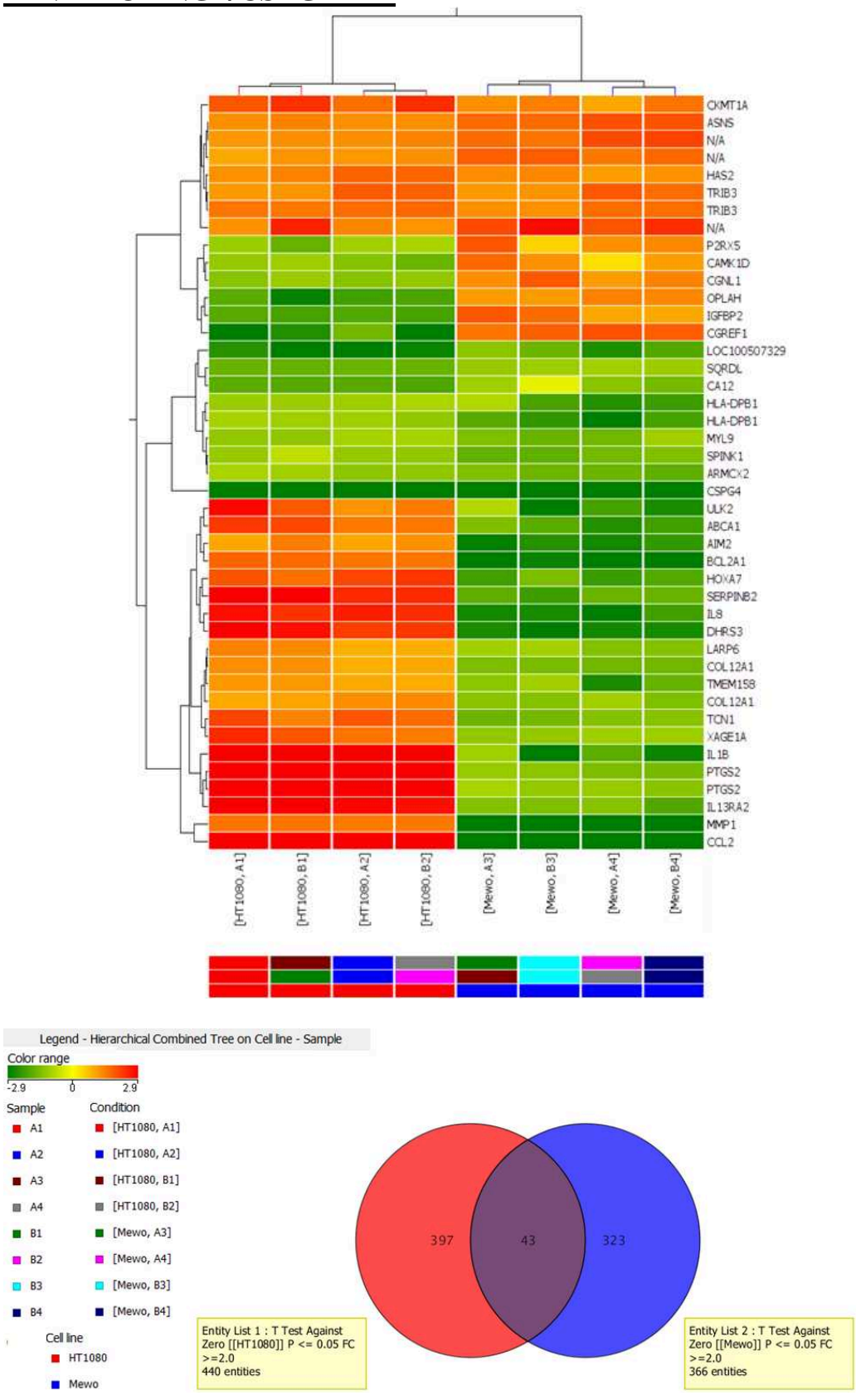

Figure 15- **DNA microarray assay on tumor mass generated by HT1080 and MeWo cells injected on nude mice.**

In order to analyzed the possible correlation between NG2/CSPG4 expression and a gene expression pattern compatible with an highly aggressive phenotype, we performed DNA microarray analysis using 4*44K Agilent whole genome platform. We made a mRNA pool from tumor mass generated by NG2 positive and NG2 negative MeWo and HT1080 cell lines injected on nude mice. mRNA was converted on cDNA and subsequently on cRNA and was hybridized to obtained cell line expression profiles. This assay shown that 397 genes were modulated only in HT1080 NG2 positive tumor mass versus NG2 negative ones, 323 only in MeWo tumor mass and 43 were commonly modulated: some are up-regulated and other are down-regulate (Figure 15). Of these 43 consensus genes, 17 were upregulated and 26 down-regulated.. Some of these gene, as MMP1 (matrix metalloprotease 1), are involved in extracellular matrix modification some other codified for structural proteins as HAS2 (hyaluronan syntase 2), other are involved in immunity response as HLA-DPB1 (major histocompatibility complex, class II, DP beta 1). So NG2/CSPG4 be correlated with a large variety of genes involved in different pathways and that indicated the complexity in studying and charactering its functions. As discussed before, cell surface expression of NG2/CSPG4 seems to correlate with a more resistant phenotype. Previous data suggested that size differences of the NG2+ and NG2- tumor masses were presumably accounted by differences in the engraftment capacities and stress-resistance capability of the two cell phenotypes.

To verify the changes of the protein expression profiles in the two tumor subtypes, we performed a phospho-proteomic screening by antibody-array that, although needing o further validation, in NG2+ subsets seems to confirm an increase of proliferation and survival pathway. In fact a lot of kinases, involved in crucial point of different signaling pathways, result to be more phosphorylated in NG2/CSPG4 positive cells than in cells without the proteoglycan as, for example, Jun kinase. The level of phosphorylation increased also in the case of FAK that is closely correlated to cell motility.

Target protein	Phosphorilation site	HT1080 Ratio NG2+/NG2-	MeWo Ratio NG2+/NG2-
PKBa (Akt1)	S473	1.61	1.51
FAK	Y576/Y577	2.04	2.90
MAPKAPK2	T222	2.02	1.59
PKA Cb	S339	2.82	2.14
PKA R2a	S99	3.88	2.58
PKCe	S729	4.08	3.65
Jun	Y170/S243	2.22/2.99	2.90/84.98
PKCq	S695	2.14	10.06
IRS1	S639	3.10	3.14

Table 4- **Common up-grade in the phosphorylation patterns in HT1080 or MeWO tumor masses**. In the table are reported the ratio between the NG2+ and NG2- subtype. Phospho-proteomic screening was performed in duplicate, on a pool of three different masses for each kind of tumors.

NG2/CSPG4 CAPABILITY TO BIND NATIVE EXTRACELLULAR MATRIX

The extracellular matrix (ECM) consists of a complex meshwork of cross-linking proteins providing both biophysical and biochemical cues that regulate cell proliferation, survival, differentiation, migration and tumor formation. ECM is a major component of tumor microenvironment and excessive deposition of ECM is a common feature of tumors with poor prognosis.

The extracellular matrix makes up a substantial part of any given tissue: it is a scaffold of proteins and polysaccharides by witch cells are supported and anchorated.

Most importantly, it is involved in providing molecular causes that regulate cell behavior.[86] The intricate relationship between the cellular and acellular components of a tissue drives its healthy development, homeostasis, and recovery from stress or injury.[87] So the vascular ECM has different functional roles which are tightly associated with its compositional and elasto-mechanic features, given them the possibility to transduce different types of signals to interacting cells. It maintains vessel architectures, serves as a growth factor storage, and in case of tissue injury (both in physiological and pathological conditions), acts as an adhesive substrate for cells of the immune system, coagulation factors, platelets and red blood cells. Vascular ECM takes place also in cancer cells extravasation and tumor progression so we focalized our attention on smooth muscle cell matrix. Nevertheless we decided to investigate cells behavior also in mesenchymal stem cell extracellular matrix because these cells constitute the precursor of pericyte, cells that plays a crucial role in vessel formation and structure.

As reported in the literature.[79,76] NG2/CSPG4 could modulate different aspects of adhesion in different tumor cell lines. Our idea was to analyzed *in vitro* the modulation of adhesion both in static condition, to verify the modulation of tumor cells' interaction with the ECM of microenvironment that could be found around the primary tumors; and in perfusion condition, to analyze the interaction between tumor cell and ECM in distant sites , typical of first metastatic steps

NG2/CSPG4 presents different binding site for extracellular matrix component: its extracellular portion is able to bind collagens as collagen IV and VI. NG2/CSPG4 itself is a component of extracellular matrix when is in its truncated form.

We re-adapted a protocol originally proposed in the late 70's to isolate cell-free native matrices from different vascular cell phenotypes and fibroblastic (stroma-like cells). The protocol was exploited both under static and perfusion and was elaborated considering mild detergent extractions to be carried out in the continuous presence of a wide spectrum of protease inhibitors. An outline of the protocol is shown in Figure 16.

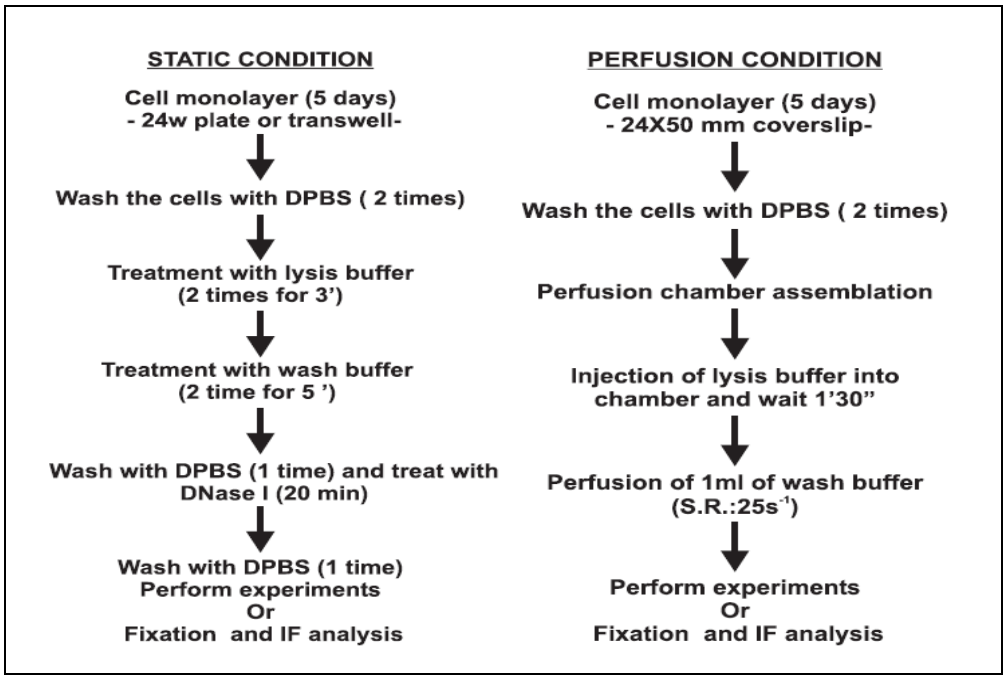

Figure 16- **Diagram of Native extracellular matrix extraction in static and dynamic condition.**

When applying the protocol, to a variety of primary and immortalized cell types, we immediately noticed a considerable variation in the quantity, topographical distribution and fragility of the isolated matrices. We then assayed a number of methods for characterizing the composition of different ECMs and their spatial distribution using different techniques biochemical and immunochemical approaches.

As a first step, we used immunostaining for fibronectin to highlight the matrix (Figure 17). It was very interesting note that each type of cell was able to produce a particular matrix with a specific and characteristic distribution of its molecules. Noticeable, although all matrices that we isolated from smooth muscle, fibroblasts and mesenchymal-type cells stained positively for fibronectin, Coll I and

Coll VI distribution of these ECM components was highly divergent in matrices isolated from the different cell types (Figure 17).

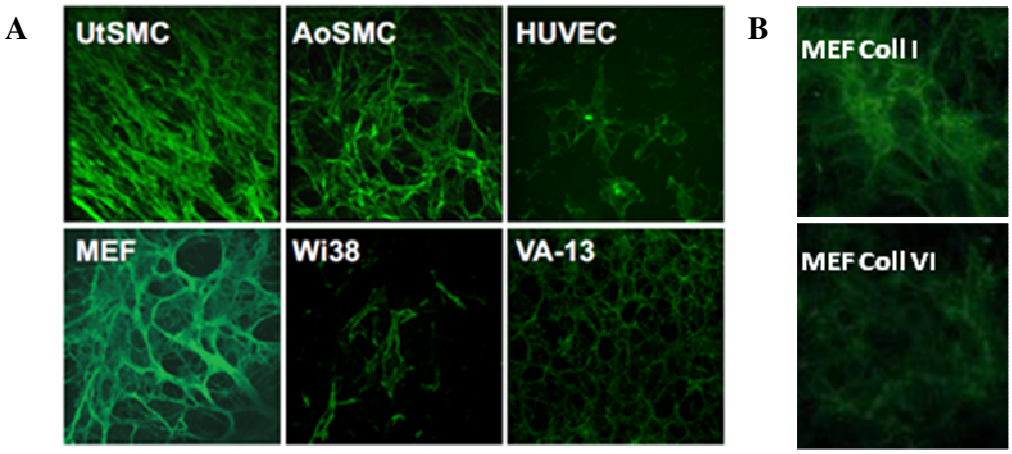

Figure 17- **Immunohistochemical assay of differet ECMs**: A) ECM were labeled with a monoclonal antibody against fibronectin; B) MEF ECM were labeled with a monoclonal antibody against Coll I and Coll VI

In the effort to fluorescently tag the isolated matrices for multi-color fluorescence analyses of the interaction of tumor cells with the isolated matrices, we tested a variety of fluorescent labelling approaches. However, none of the currently known fluorescent protein dyes could be exploited as in most cases the procedure for tagging the matrices with these dyes involved chemical modification of the matrix. We therefore turned to the use of a chemical metabolic labelling procedure based upon a chemoselective ligation strategy (one component of the reaction used as an analog of a naturally occurring molecule that is required for catabolism of a target macromolecule). In particular, we used synthetic amino acids and sugars that can be incorporated during protein synthesis and post-translational glycosylation using the intrinsic metabolic machinery of the cell.

We then cultured cells with the specific chemoselective ligand, isolated the matrix and analyzed it by confocal laser microscopy. The approach effectively highlighted the overall organization of the matrix deposited by vascular cells in culture (Figure 18).

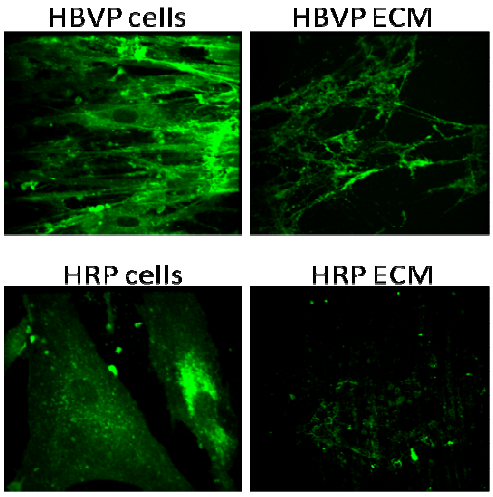

Figure 18- **In vivo metabolic labeling assay**: on the left there are imagines of whole human brain vascular pericyte cells (HBVP) and immortalized retinal pericytes (HRP); on the right the relative extracellular matrix.

Further analyses of the isolated matrices were performed by SDS-PAGE under reducing and non-reducing conditions and labeled with silver staining (Figure 19).

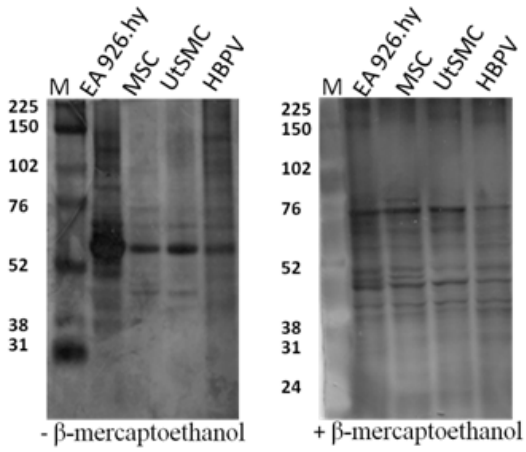

Figure 19- **Silver staining of ECMs** obtained from the indicted cell lines and resolved by SDS-PAGE under reducing and non-reducing conditions.

The different migration pattern were obtained but we will made mass spectrometry assay to complete matrices characterization and AFM and e-SEM assay are ongoing in order to obtain a matrix topography.

In a second phase we decided to made a functional study testing the capability of tumor cell, immunosorted for CSPG4/ NG2, to migrate through different ECM proteins coated on transwell system at the final concentration of 20 ug/ml. It was usefull, in fact, to analyze the phenomana on a simple system before tested the cellular adhesion on native ECM. This step was very important to understand the interaction dynamics that regulate the cell migration and colonization of tissues: descover if tumor cells prefer to interact whit some ECM component could be a way to urderstand the dymanics that drive metastasis formation.

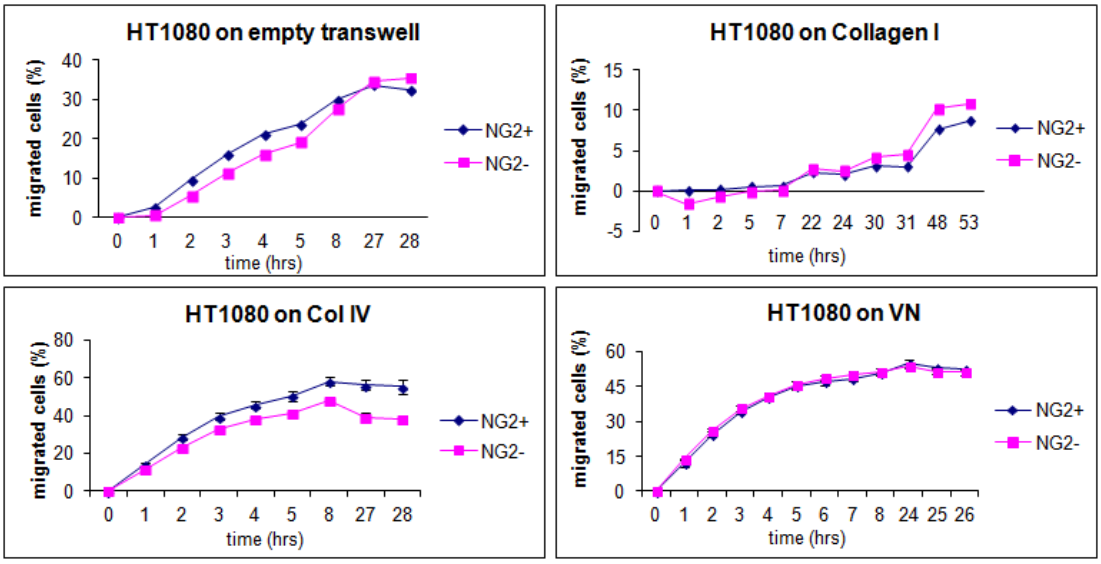

Figure 20- **Migration assay**: singular extracellular matrix component were coated on transwell surface at the concentration of 20 ug/ml in bicarbonate buffer, in a humid chamber and at 4°C over night.

The HT1080 NG2+ and NG2- subpopulation were tested on different ECM components as fibronectin, vitronectin, Collagen I, III, IV, VI, VIII and laminin, empty transwell was used as a control (Figure 20). However we observed a different capability to pass through the transwell just in the case of collagens I and IV. In particular HT1080 NG2+ subpopulation are more able than HT1080 NG2- one to pass the collagen I coat, on the other size the HT1080 NG2- cells shown a better capacity to pass through the collagen IV coat. Probably the capability to migrate correlates with a less avidity in bind the coated ECM component. It is well known, in fact, that microenvironment is determinant in tumor cells dissemination, growth and capability to colonize different body districts.

In order to analyze the interaction between tumor cell and ECM in distant sites , typical of first metastatic steps, we tested the same cell subpopulations under flow conditions. Cells were perfused on different ECM components coated (in the same experimental condition described for in static proves) using a 50 sec^{-1} shear rate. We analyzed cell adhesion and aggregation after 5 and 10 minutes of flow because we noticed a logarithmic increase in a time dependent way.

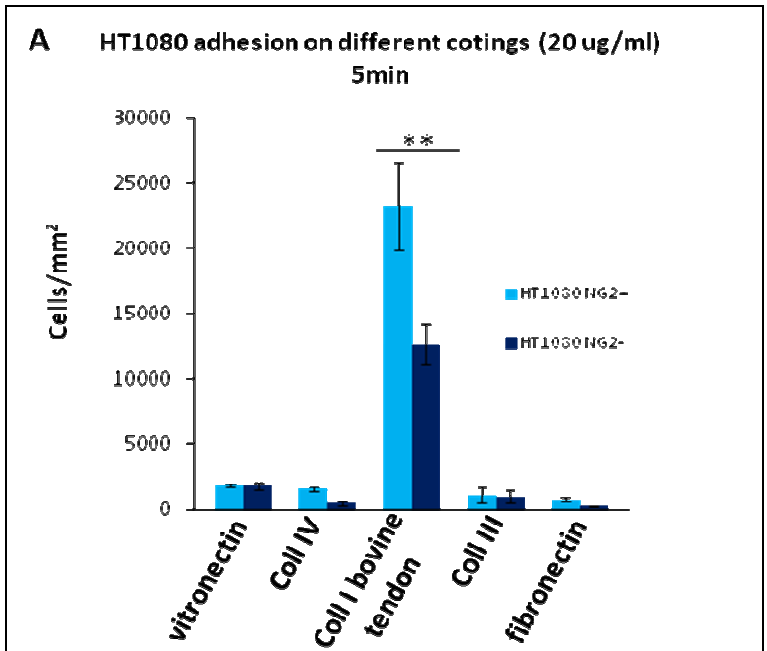

B

HT1080 adhesion on different cotings (20 ug/ml) 5min

		1 cell	2 cells	3 cells	4-6 cells	>6 cells
FN 20ug/ml	HT1080 NG2 +	90%	10%	0%	0%	0%
	HT1080 NG2-	67%	23%	5%	5%	0%
VN 20ug/ml	HT1080 NG2+	70%	10%	10%	7%	3%
	HT1080 NG2-	5%	9%	8%	18%	60%
Coll IV 20ug/ml	HT1080 NG2+	8%	14%	7%	18%	53%
	HT1080 NG2-	91%	4%	3%	1%	0%
Coll I 20ug/ml	HT1080 NG2 +	88%	11%	2%	6%	11%
	HT1080 NG2-	54%	15%	12%	15%	4%

Figure 21- **Sarcoma adhesion and aggregation assay on different coating after 5 min of perfusion:** A) Adhesion assay permit to evaluate the cell number for mm^2; (*:p<0.5; **:p<0.05; ***:p<0.005). B) Aggregation assay permit to evaluate the percentage of aggregates based on cell number for each cluster

No important differences were noticed between the two HT1080 immunosorted subpopulation except in case of Collagen type I from bovine tendon, a macrofibrillar form: in this case NG2 appears to confer to the cell a best affinity for this component as shown by adhesion ad aggregation assay (Figure 21).

Similar results were obtained with immunosorted MeWo cells: MeWo NG2+ subopulation adhere better than MeWo NG2- ones on Collagen type IV (Figure 26)

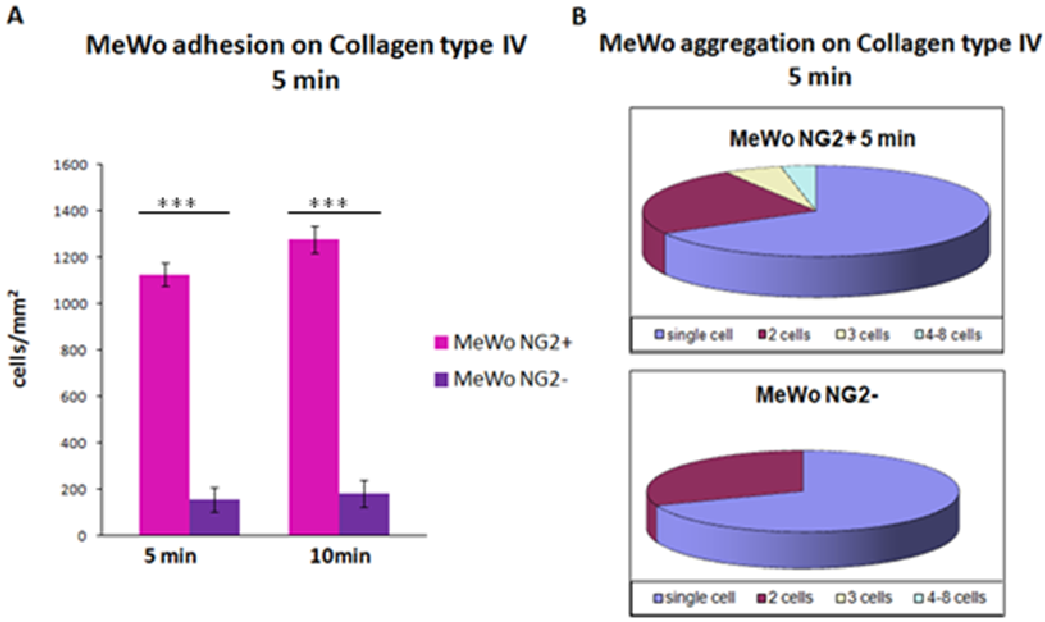

Figure 22- **Melanoma cells adhesion and aggregation assay on Collagen type IV after 5 min of perfusion**: A) Adhesion assay permit to evaluate the cell number for mm^2; (*:p<0.5; **:p<0.05; ***:p<0.005) B) Aggregation assay permit to evaluate the percentage of aggregates based on cell number for each cluster

To evaluate NG2/CSPG4 effect on cell adhesion and migration through the ECM it seems necessary a more specific system able to mimic the vascular ECM different functional roles which are probably tightly associated both with its compositional and elasto-mechanic features. In order to better investigate this aspect we decided to use a synthetic ECM, matrigel growth factor reduced, and we made a 1,5 mg/ml preparation coated on a cover-slip glass. We perfuse both HT1080 and MeWo immunosorted cells: NG2/CSPG4 could be favor cell adhesion even if no clear cut results were obtained (Figure 23). So it was necessary to study the cell behavior on native extracellular matrix.

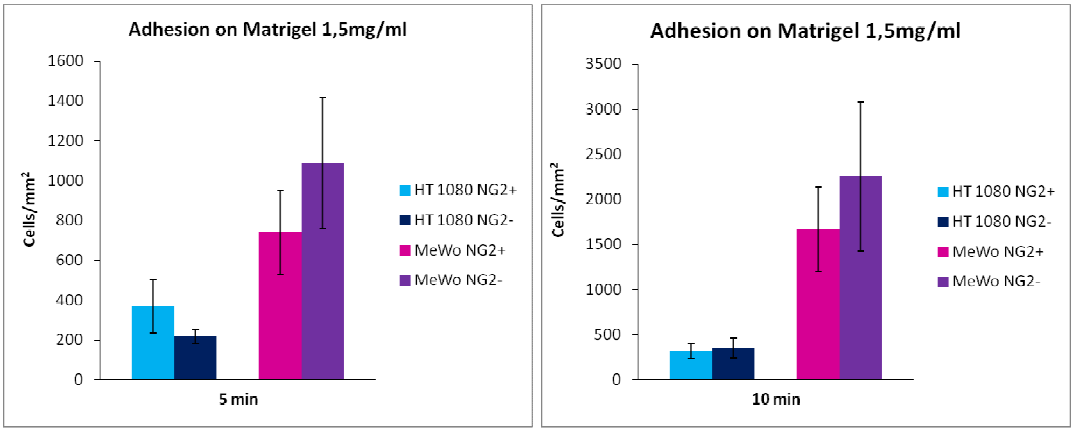

Figure 23- **Cell adhesion on Matrigel Growth factors deduced:** cell count was made at 5 and 10 minuts

We decided to made the same experiments on native extracellular matrix obtained from smooth muscle cells and from mesenchimal stem cells. The choose of these two cells line wasn't casual: smooth muscle cells are a crucial component of vessels and mesenchimal stem cells are able to produce a matrix that could present common characteristics to different tissue because these cells are able to differenciate in a large variety of other cells. On the other hand the vascular ECM maintains vessel architectures, serves as growth factor storage, and in case of tissue injury (both in physiological and pathological conditions), acts as an adhesive substrate for cells of the immune system, coagulation factors, platelets, red blood cells and tumor cells.
After 5 days of cell confluence we used our extraction protocol to obtain the native ECM. For the migration assay HT1080 immunosorted cell line were plated on transwell system and we rated the percentage of cells able to pass trough the pores in 24 hours.

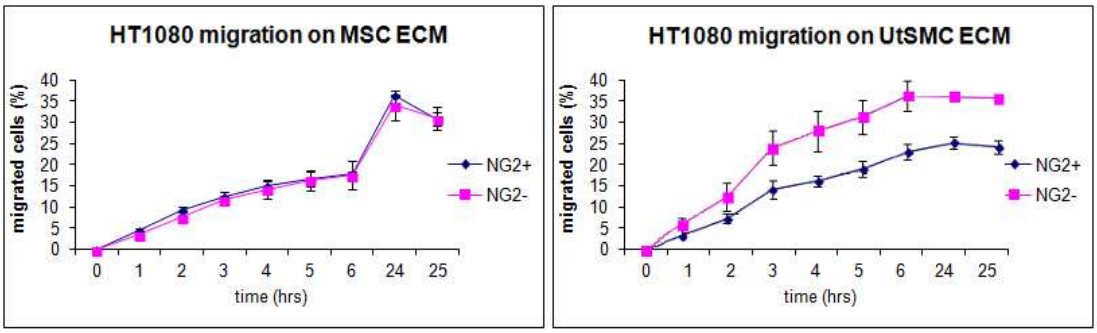

Figure 24- **Sarcoma cells migration assay**: native extracellular matrices were obtained on transwell surface and cell count was made after 24 hours from seeding.

On UtSMC ECM the HT1080 NG2+ appeared to be more able than HT1080NG2- to migrate, instead on MSC ECM no differences were noticed (Figure 24). HT1080 subpopulation cells were also tested on dynamic condition and in this cas we rate the cell adhesion and the cell aggregation. ECM were obtained directly into the flow chamber and sarcoma cells were labeled and perfused on ECM. The cell count was made after 5 and 10 minutes of perfusion.

These experiments demonstrated that cell adhesion to native ECM varied according to cell type from which it was derived: HT1080 NG2+ subpopulation adheres more than HT1080 NG2- one to UtSMC matrix, the opposite hapened on MSC matrix (Figura 25 A). The aggregation assay shown that both NG2 positive and negative cells adhere better on MSC than on UtSMC ECM (Figura 25).

A

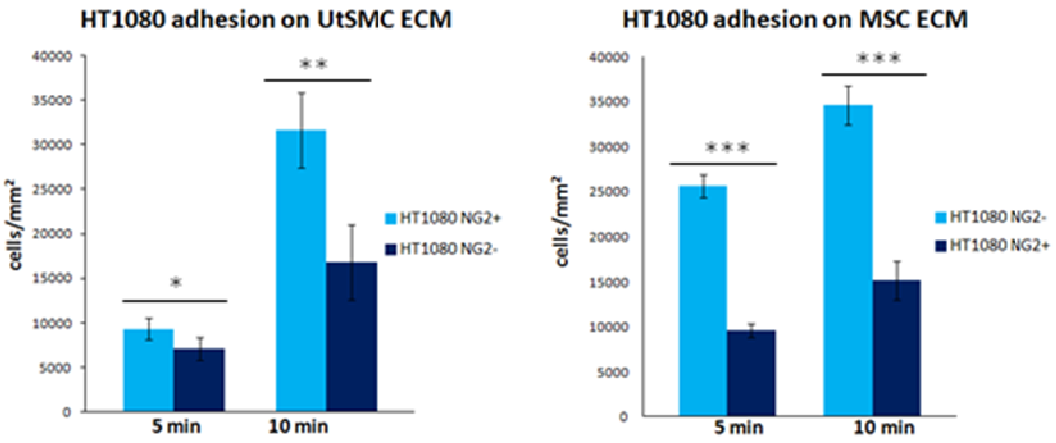

B

HT1080 aggregation on different Extracellular Matrix

		1 cell	2 cells	3 cells	4-6 cells	>6 cells
ECM UtSMC	HT1080 NG2 +	34 %	11%	9%	17%	29%
	HT1080 NG2-	45%	18%	13%	16%	8%
ECM MSC	HT1080 NG2+	5%	9%	8%	18%	60%
	HT1080 NG2-	8%	14%	7%	18%	53%

Figura 25- **Sarcoma cells adhesion and aggregation assay on UtSMC and MSC ECM after 5 min of perfusion**: A) Adhesion assay permit to evaluate the cell number for mm^2; B) Aggregation assay permit to evaluate the percentage of aggregates based on cell number for each cluster

In order to confirm these data MeWo immunosorted cells were tested in the same experimental condition both for adhesion and aggregation and they shown the same cellular behavior of sarcoma cells (Figure 26).

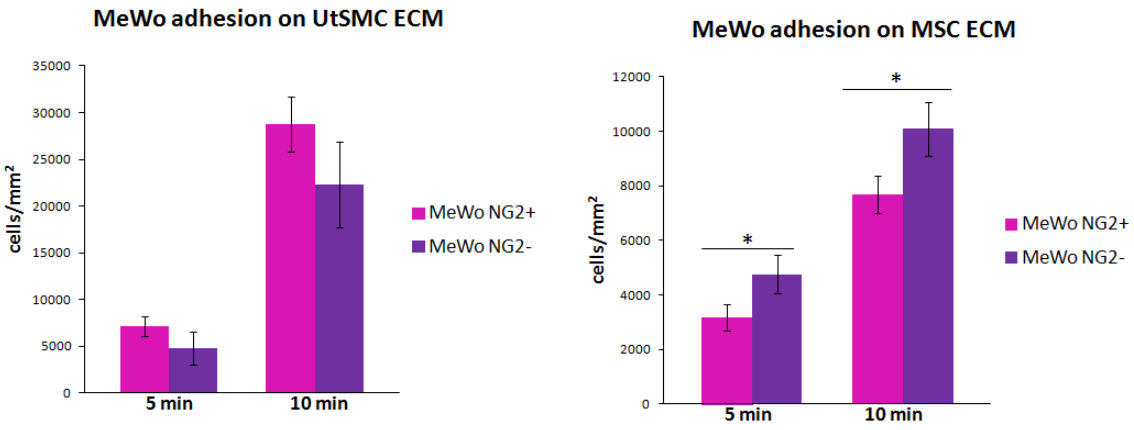

Figure 26- **Melanoma cells adhesion and aggregation assay on UtSMC and MSC ECM after 5 min of perfusion**; (*:p<0.5; **:p<0.05; ***:p<0.005)

NG2/CSPG4 MEDIATES TUMOUR CELL BINDING TO THE ENDOTHELIUM

Adhesion of circulating cells as tumor cells to intimal endoyhelial cell monolayer is throught to be one of earliest events in metastatis formation. Using a perfusion system (Figure 27) formed by a peristaltic pomp able to mimic the reologycal conditions of blood in small vessels connected with a the perfusion parallel-flow chamber, we were able to simulate the shear stress and shear force that guide the cells perfusion in blood microcirculation. In the perfusion chamber it is possible to assemble a cover-slip glass with a cell monolayer on the top. The assembled perfusion chamber could be can be mounted in the slot on the table of the inverted microscope. Thanks to a camera it is possible to record each part of the experiment and made a video.

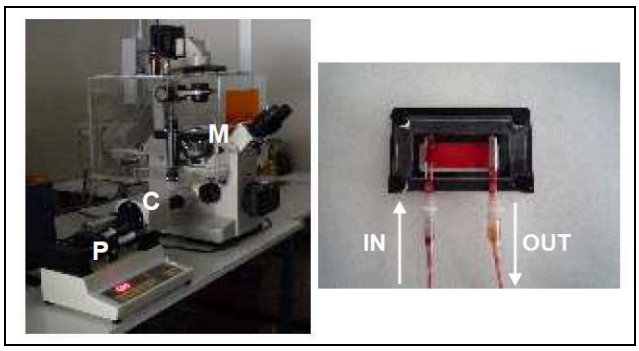

Figure 27 - **Set up for perfusion experiments**: *left panel* shows the pump *(P)* and video-camera *(C)* connected to an inverted microscope *(M)*, whereas *right panel* shows the perfusion parallel-flow chamber assembly with the collection tubings. The inner tube on the left (*IN*) permits the access to the HT1080 cell suspension into the chamber; the tube connected to the pump (*OUT*) on the right is intended for the aspiration of the perfused liquid. *Arrows* indicate the direction of the applied flow.

In the subsequent experiments we examine the effect of TNFα on cultured human umbilical vein endothelial cell (HUVEC) and on the same cell line immortalized (EA926.hy). First we tested the effect of TNFa to activate endothelial cells and the followed capability of differet cell lines, selected on the NG2/CSPG4 positivity, to interact with endothelial cell before and after attivation.

HUVEC cells were treated with TNFα 10ng/ml in medium serum free for 4 hour at 37 °C to activated them. After this period they were put in flow system to be tested under shear stress condition. Perfused cells were labeled with DiI and

resuspended in serum free medium at the final concentration of $1*10^6$ cells/ml. The perfusion condition provides shear rate was 50 sec^{-1}.

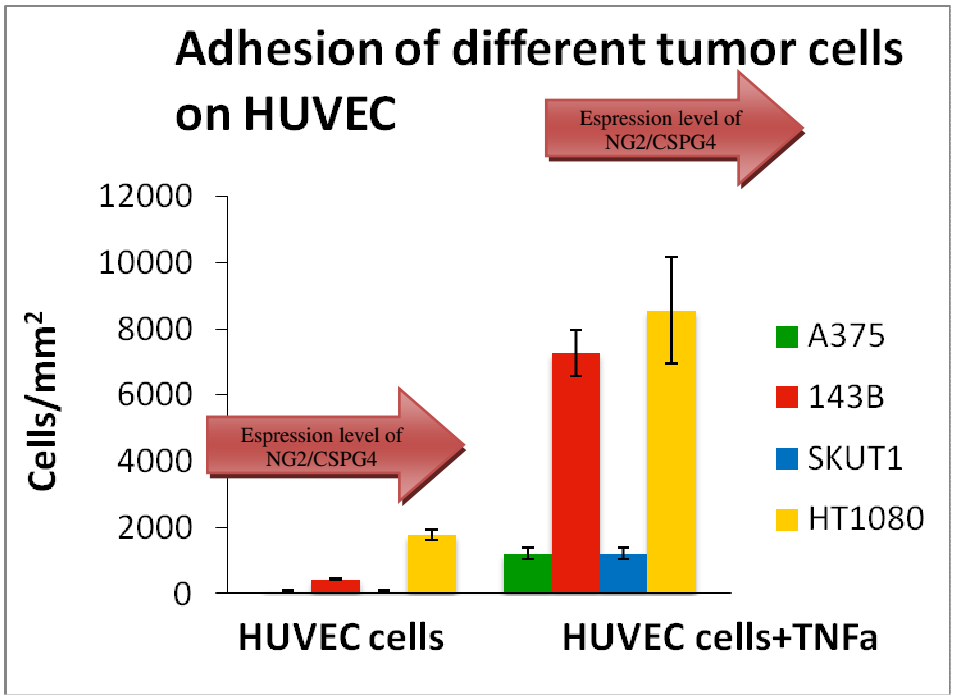

Figure 28- **Behavior of different cell lines expressing differet levels of NG2 on their cell surface tested on HUVEC cells attivated 10 ng/ml TNFa or not activated on reological condicions**. The NG2/CSPG4 level were estimated by FACS analysis.

As could be expected, flowing tumour cells bound more tenaciously to activated endothelial cells than to untreated one. After 5 minutes of perfusion, the HT1080 NG2+ subpopulation was observed to adhere better than the corresponding one to the endothelium. The extent of ell-cell aggregation observed in HT1080 NG2+ and NG2- differed primary for the higher degree of clusters including 4-8 cells (Figure 28). The same trends were shown after 10 minutes of perfusion (data not shown).

Because of technical limitations with primary endothelial cells, we turned to an immortalized endothelial cells, EA926.hy cells. This cell line was generated by fusion oh HUVEC with the human lung carcinoma cell line A549. The resulting hybrids are contact inhibited in growth, shown reduced growth factor requirements, express vWF and upregulate ICAM-1, V-CAM 1 and E-selectin expression upon stimulation with TNFα[88]. EA 926.hy has been used for adhesion assays with several human cell lines as leukocyte, peripheral blood mononuclear cells and neutrophils.

Testing of the immunosorted sarcoma cell lines we obtained sigenerated by perfusion on HUVEC cells line.

In order to better understand the effect of NG2/CSPG4 presence on cell surface on adhesion under flow condition, we analyzed the behavior of immunosorted HT1080 cells line in a 10 minutes time score. In the same experiment we analyzed also the cell aggregation capacity.

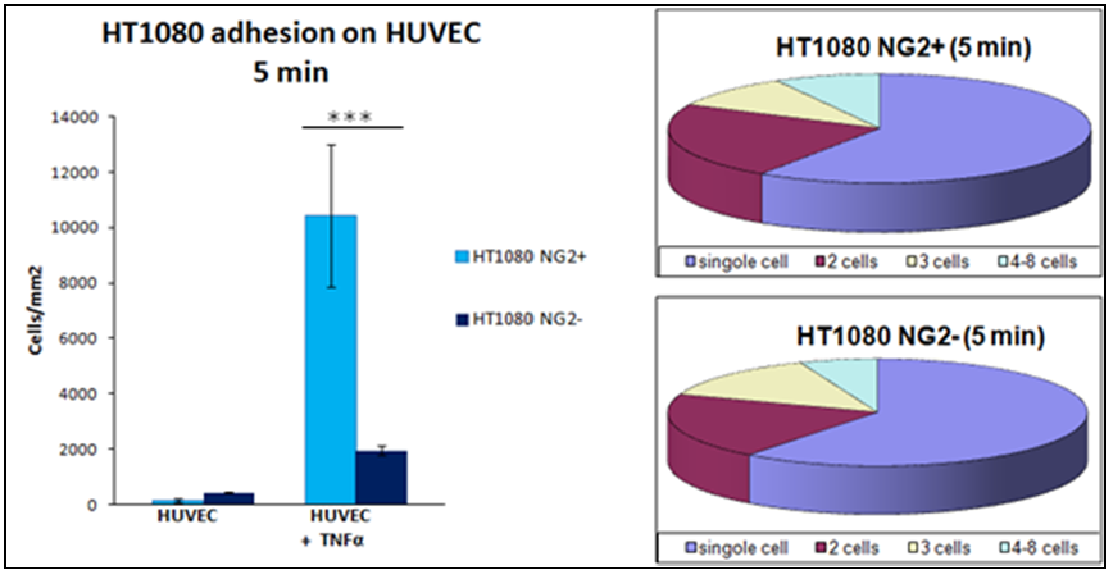

Figure 29- **Adhesion and aggregation assay**: HT1080 NG2+ and NG2- subpopulation were perfused on HUVEC cells treated or not with TNFα (10 ng/ml) for 4 hours at 37°C and 5% of CO_2; (*:p<0.5; **:p<0.05; ***:p<0.005). Cells and aggregates were counted after 5 minutes of perfusion using CellCounterBL Program.

After 5 minutes HT1080 NG2+ subpopulation adhere better than HT1080 NG2- one. In particular, the NG2 positive subpulation adhere approximately 10 time more than the negative ones. No differences were noticed on aggregation assay: almost all cells occur as a single cell, and most of the aggregates is 2 or 3 cells cluster and this phenoma seems to be not correlate to the TNFα effect (Figure 29). The same trends were shown after 10 minutes of perfusion (data not shown).

In vitro studies on the role of the endothelial cell in cell adhesion are hampered by the difficulty in reproducibly obtaining the large numbers of endothelial cells required for such studies because the life span of endothelial cells in culture is limited and because endothelial cell properties can change during culture. The availability of permanent endothelial cell lines that retain differentiated endothelial characteristics might be of benefit in this respect.

For all these motifs we decided to investigate the cell behavior on immortalized endothelia cells, EA926.hy cells. This cell line was generated by fusion on HUVEC with the human lung carcinoma cell line A549. The resulting hybrids are contact inhibited in growth, shown reduced growth factor requirements, express vWF and upregulate ICAM-1, V-CAM 1 and E-selectin expression upon stimulation with TNFα [88]. EA 926.hy has been used for adhesion assay with several human cell lines as leukocyte, peripheral blood mononuclear cells and neutrophils. Testing the same sarcoma immunosorted cell lines we obtained similar results generated by perfusion on HUVEC cells line (Figure 30).

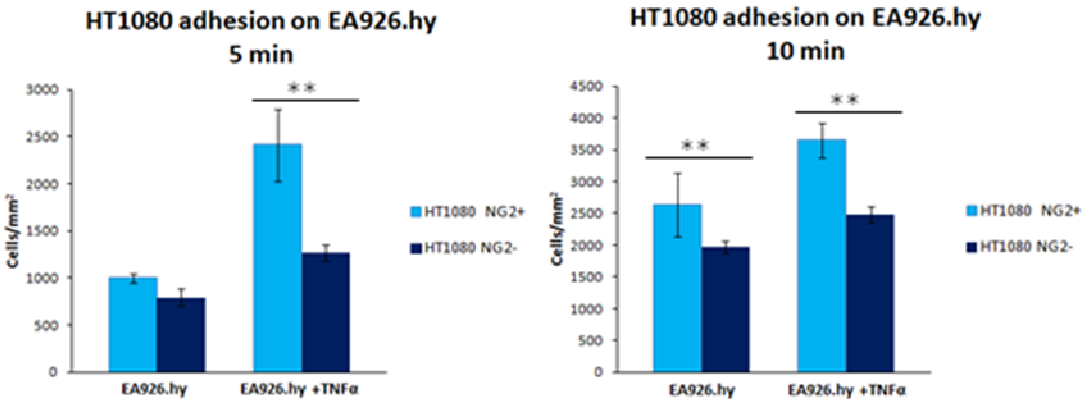

Figure 30- **Adhesion assay**: HT1080 NG2+ and NG2- subpopulation were perfused on EA 926.hy cells treated or not with TNFα (20 ng/ml) for 4 hours at 37°C and 5% of CO_2; (*:p<0.5; **:p<0.05; ***:p<0.005). Cells and aggregates were counted after 5 and 10 minutes of perfusion using CellCounterBL Program

We will better investigate what kind molecules could be involved setting other experiment in the future. HT1080 immunsorted cell were tested also in static conditions and in particular we want to investigate their capacity to migrate across the endothelia monolayer grown in a transwell system. It is well known that the endothelial layer requires specific organization including a requisite apical–basolateral polarity corresponding to luminal and abluminal membranes. Coincident with providing a barrier to flow, the endothelial layer also functions to regulate permeability. To mimic the endothelia cell polarization we coat HUVEC cells on the top (mimic intravasation) or on the bottom (mimic extravasation) of the transwell and we use complete medium to stimulate tumor cells, put on the upper chamber, to

migrate across the endothelia monolayer. However our experiment didn't show any differences in cell migration due to the endothelia polarization (Figure 31).

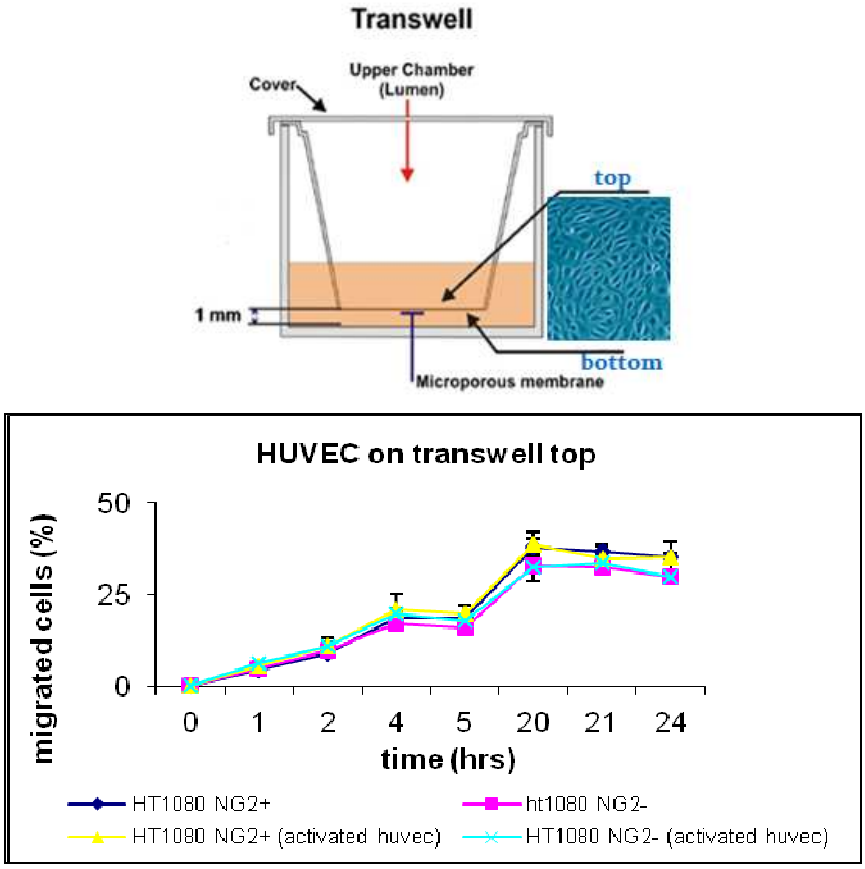

Figure 31- **Migration assay**: A) Transwell system rappresentation; B) a HUVEC cell monolayer were coated on transwell surface and tumor cells expressing different NG2/CSPG4 levels were seeded on the upper chamber. Compete medium was used as a chemoattactant factor. The analysis was made in a 24 hours period

NG2/CSPG4 INTERACTS WITH MICROENVIROMENTAL FACTORS ALSO THANKS TO ITS CHONDROITION SULFATE CHAINS

To try to better understand the role of NG2/CSPG4 chondroitin sulfate chain in cell adhesion on endothelia, tumor cells presenting NG2 were treated using 0,2 U/ml Chondroitinase ABC. As shown by FACS analysis (Figure 32 A), after treatment, cells didn't expose any chondroitin-sulphate chain and this indicated the successful of digestion. Immunofluorence assay using a monocolonal antibody against condroitin sulfate chains shown that the endothelia digestion was successful too (Figure 32 B).

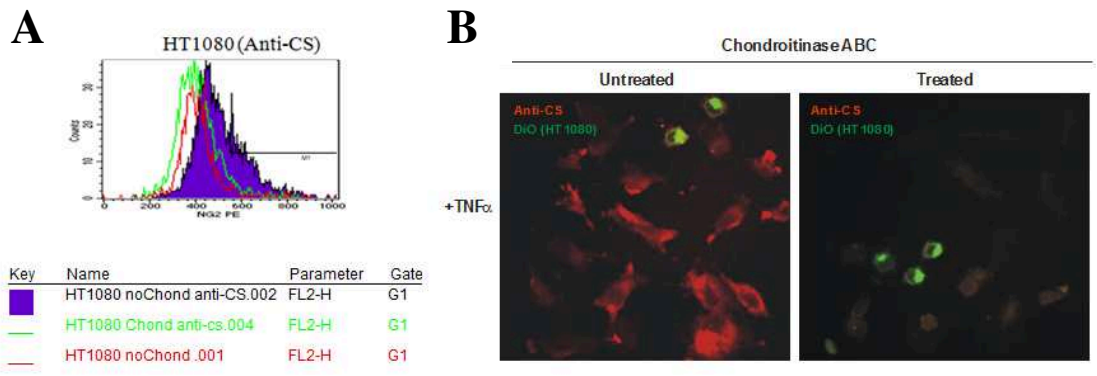

Figure 32 - **Chondritin sulfate levels**: A) FACS analysis for evaluate the chondroitin sulfate levels on cell surface; B) immunoistochemical assay to evaluate the happened digestion of chondroitin sulfate after enzymatic treatment

Testing HT1080 NG2+ subpopulation on non activated, on TNFα treated and on TNFα and Chondroitinase ABC treated HUVEC cells on rheological condition it was possible to notice that after chondroitin sulphate clever, both on tumor cell surface and on endothelial cells, the cell adhesion markedly decreases both at 5 and 10 minutes of perfusion (Figure 33 A).

A

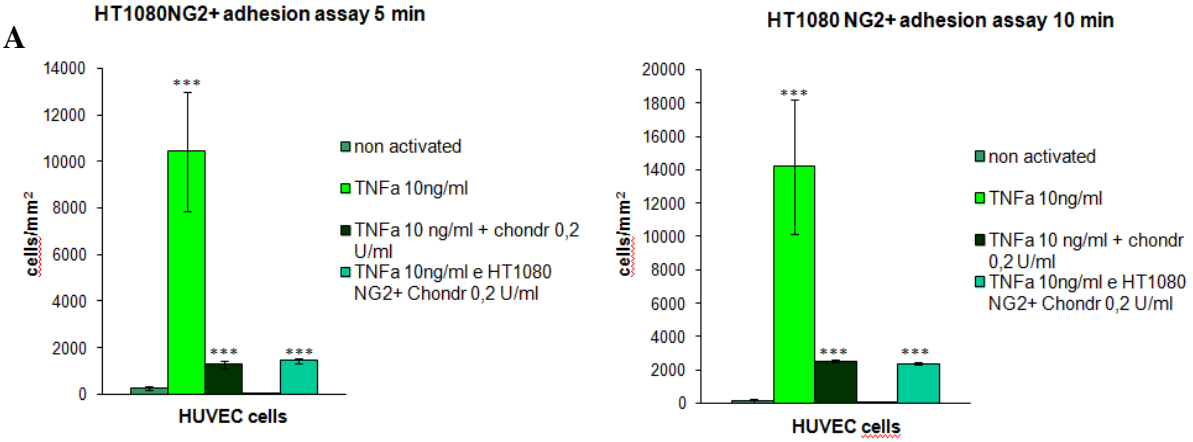

B

		1 cell	2 cells	3 cells	4-8 cells
EA926.hy +TNFα	HT1080 NG2 +	59%	23%	10%	8%
	HT1080 NG2+ ChondABC	86%	12%	2%	0%
EA926.hy +TNFα + ChondABC	HT1080 NG2 +	83%	12%	5%	18%

Figure 33- **Adhesion assay under flow condition**: A) HT1080 NG2+ cells were tested on activated and not activated and on Chondroinase ABC treated endothelia cells (lines 1,2 and 3). HT1080 NG2+ cells treated with the same enzyme were tested on activated endothelia (line 4).(*:p<0.5; **:p<0.05; ***:p<0.005) B) Aggregation assay in the same experimental condition and with the same cells of adhesion proves.

Chondroitin sulfate cleavage influence also the cell aggregation: after treatment on endothelium tumor cells aggregation power is comparable to the cell behavior shown on non activated endothelium. The same effect was noticed treating tumor cells with Chondroitinase ABC (Figure 34). This suggests a involvement of cell surface chondroitin sulfate in cell-cell interaction . Experiments performed with HUVEC were reproduced with the immortalized EA926.hy cell line, obtaining comparable results.

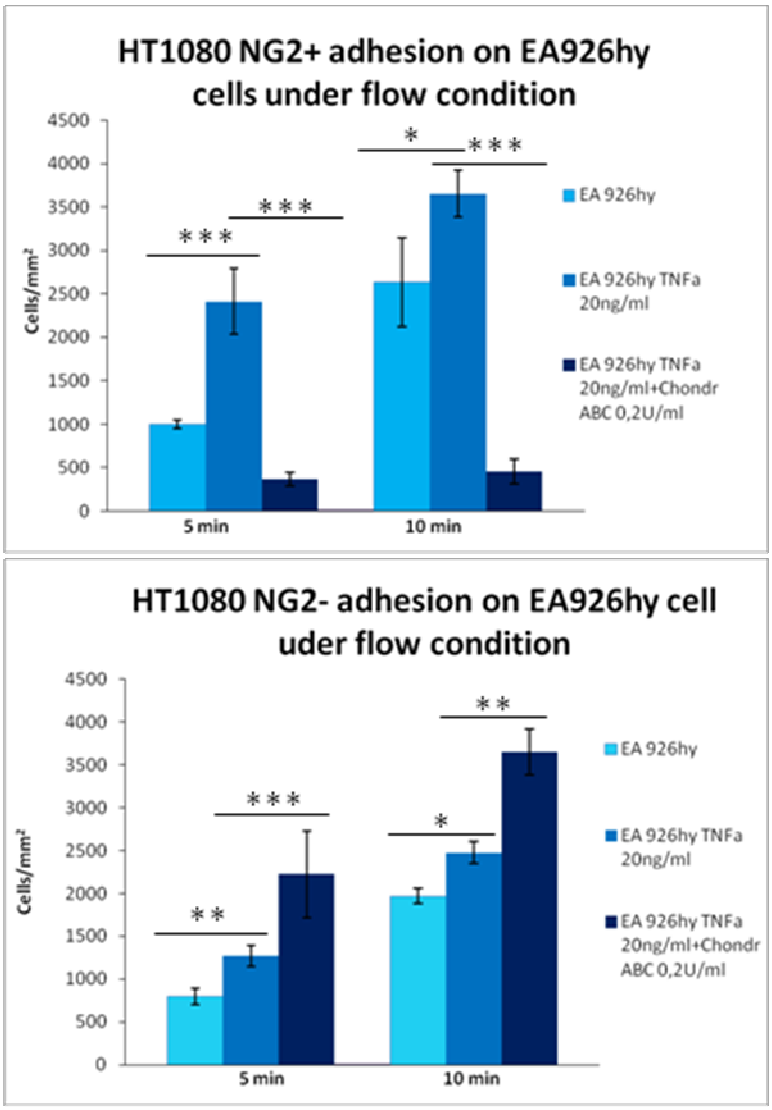

Figure 34- **Adhesion assay on non activated, activated and Chondroitinase ABC treated immortalized endothelia cells:** both HT1080 NG2+ and NG2- cells were tested; (*:p<0.5; **:p<0.05; ***:p<0.005)

Different results was obtained testing the HT1080NG2- subpopulation: in this case the Chondroitinase ACB treatment seemed to cause a further increase of the adhesive capacity of tumor cells (Figure 34). This could suggest a potential involvement of some chondroitin sulfate chain present on endothelia in tumor cell attract, catch and adhesion.

LOSS OF NG2/CSPG4 CAUSE A DECREASE IN CELL ADHESION POTETIAL

To further address the role of NG2/CSPG4 proteoglycan in control of tumor cell adhesion we abrogate its expression using siRNA probe mechanism. We made this experiment on MeWo cells because they present constitutively appreciable levels of NG2 on their cell surface. To enhance the proteoglycan presence we used MeWo NG2+ cells and we were able to obtained a 30% silenced population, as shown by FACS analysis (Figure 35 A). Treated cells were tested on activated and not activated immortalized endothelia cells under flow condition to verify their adhesion capabilities.

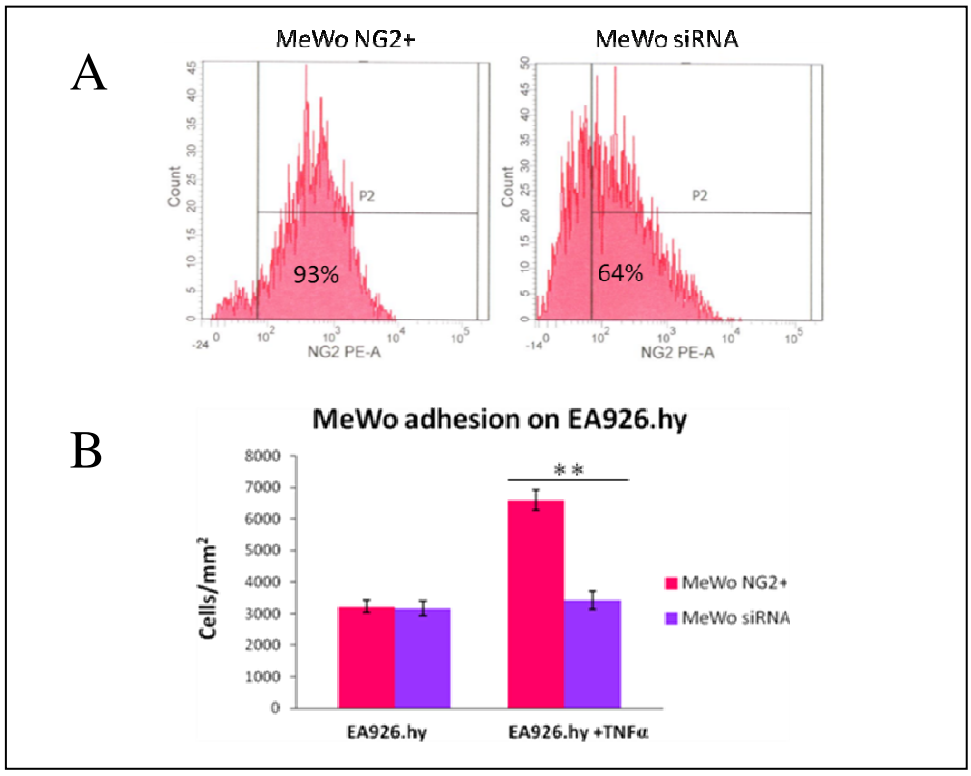

Figure 35- **NG2/CSPG4 abrogation**: A) FACS analysis after silencing: B) functional study of silenced cell to value their adhesion potential after 5 min. of perfusion; (*:p<0.5; **:p<0.05; ***:p<0.005).

It was found that on TNFα activated endothelial cells the NG2/CSPG4 abrogated cells shown lower level of adhesion than non abrogated one and this decrease was strictly correlated with the efficiency of PG abbroagaton: silenced cells adhere 40-50% time less than non abrogated cells (Figure 35 B). For the future we want to improve our knowledge in NG2/CSPG4 roles continuing in cells silencing experiments and testing other cell lines.

NG2 INFLUENCES NEOVASCULARIZATION

The CAM angiogenic response implemented by cell lines HT1080 $NG2^+$ and HT1080 $NG2^-$ shows similar result, which is a strong neo-vascular formation in support of the inoculum (Figure 36). Regarding tumor dissemination, the cell line HT1080 $NG2^+$ gives a massive intravasation compared to a lesser one of HT1080 $NG2^-$ cells (Figure 36).

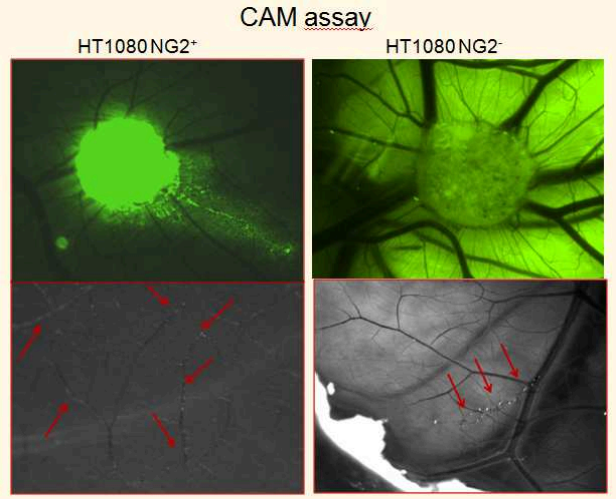

Figure 36- **Microscopical images of human tumor cell graft on chicken embyos**

To investigate the cell invasiveness we made a molecular analysis of human specific DNA detecting ALU sequences in the DNA samples from CAM and chicken embryos. As expected, a band is present in CAM proximal samples inoculated with either HT1080 NG2+ and HT1080 NG2- cells. Another band is present in the sample of distal CAM inoculated with HT1080 $NG2^-$ instead there is a band in sample of organs inoculated with HT1080 NG2+ (Figure 37).

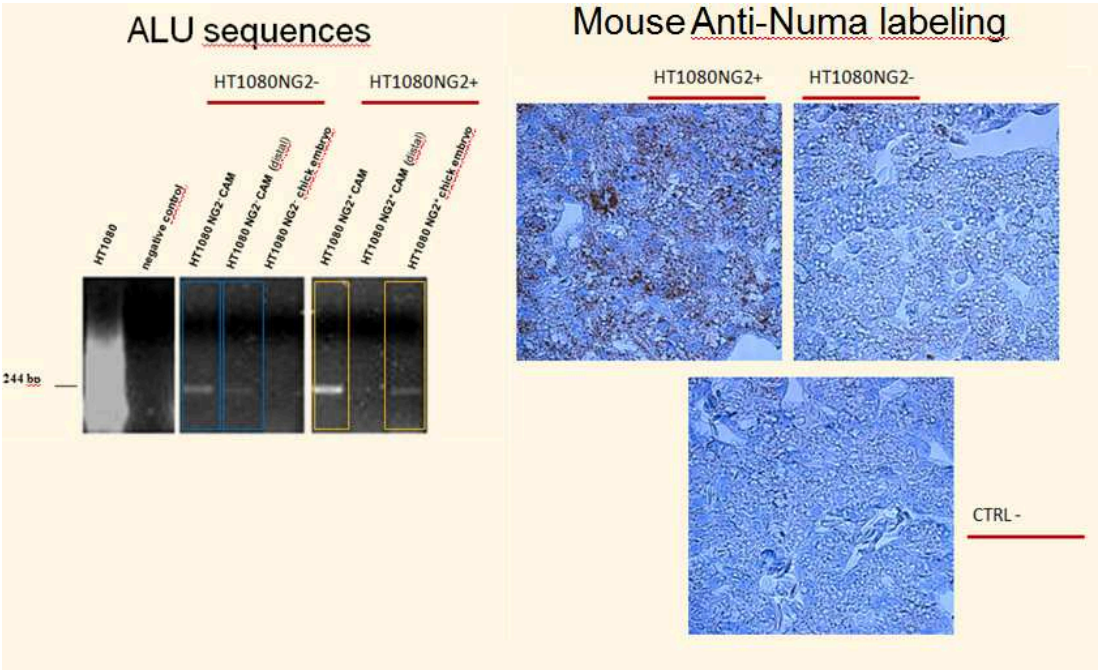

Figure 37- **Detection of human tumour cells in CAM assays:** A) Human ALU sequence detection in CAMs receiving human tumour cell implantations; B) Immunohistochemical assay on embryo's liver sections using a human-specific antibody angains Numa

The same embryo's parts were tested by immunohistochemical analysis in order to identify tumor cell infiltration. As shown in liver sections, HT1080 NG2+ cells shown high invasiveness power if compared to HT1080 NG2- cells (Figure 37). In our preliminary experiments we shown that HT1080 NG2- cells weren't able to pass the CAM barrier and they move on it, on the other hands HT1080 NG2+ ones are able to invade embryo chicken organs. All these data are in accord to *in vitro* studies that demonstrated the higt aggressive power conferred to cells by NG2/CSPG4 presence and to *in vivo* observation: tumor that present this proteoglycan shown a bad prognosis.

DISCUSSION

The metastatic cascade entails an initial step in which tumor cells intravasate lymphatic or haematic circuits and develop the ability to interact with the endothelium of distant sites, followed by a subsequent interaction with the underlying ECM to pursue their tissue infiltration. To explore more in detail some of these metastatic passages and address the role played by membrane-bound proteoglycans (PGs), we have devised an experimental paradigm that allows us to investigate how these PGs may directly or indirectly affect cell-cell and cell-ECM interactions in settings that mimic *in vitro* the rheological conditions encountered by tumor cells in peripheral blood.

NG2/CSPG4 cell surface proteoglycan represents a novel independent prognostic factor in certain types of soft-tissue sarcomas where its relative expression levels in primitive lesions strongly predict future appearance of metastases. Starting from this observation we screening different cell lines for the presence of NG2 using FACS analysis and then we tested the same cell lines with scratch assay on plastic without coating to observe their capability to move. We noticed that high levels of NG2 on cell surface, as happened in some melanomas, seems to correlate with a less efficient cell capability to move: so in presence of this proteolglycan cells are more able to establish contacts with the microenvironment and their bind is stronger than tumor cells showing low levels of NG2. In a second moment we tried to separate, starting from the same cell population, cells that presented the proteoglycan we were studying from cells who didn't present it. So we were able to obtained two subpopulation one enriched for NG2/CSPG4 presenting cells (NG2+) and the other one enriched for cells without NG2/CSPG4 on their membrane (NG2-) for sarcoma cell line HT1080 and for melanoma cell line MeWo. When we comparatively assayed the tumorigenic behaviour of immunosorted cells in nude mice, we found that the former subset gave rise to local tumor masses more rapidly and more extensively than the latter one. This observation was consistent with corollary in vitro findings: testing these immunosorted cell line we could demonstrate that the presence of NG2/CSPG4 mediates growth under stress condition. In fact NG2+ subpopulation shown a more aggressive phenotype than NG2- subpopulation: they survival more under starvation and overconfluence conditions and they proliferate more as demonstrated by soft agar assay.

Expression of surface PGs significantly accentuated binding of tumor cells to microenvironment molecules. By cooperating with integrins, or by direct binding to extracellular ligands, in fact, NG2 is believed to affect filopodia extension and stabilization and activate lamellopodial signaling cascades propagated via p130CAS, Rac/cdc42 and FAK-ERK phosphorylations.[89,64] The NG2-induced rearrangement of the actin cytoskeleton may occur through ancillary actin-binding intermediates and more recently syntenin-1 has been added to the list of putative NG2-cytoskeletal linker/adaptor molecules in migrating oligodendrocytes.[90] . Modulation of the phosphorylation state of molecules affecting the actomyosin-regulated cell contractility and focal adhesion formation provided additional evidence for a tight NG2 exerted control of the actin microfilament dynamics in critical cytoplasmic domains of motile cells. NG2 may also influence focal adhesion disassembly and the dynamics of the retracting end apparatus of locomotory cells.

Moreover, the expression of NG2 could modulate the tumor cells' behavior in haptotatic movement as well as in scratch assay or in 3D movement. When stimulated to migrate using a chemoattractant, as viewed on matrigel evasion test, NG2- cells migrate better then NG2+ ones. NG2/CSPG4 proteoglycan seemed to be involved in injury heal: cells that expose it on their surface covered faster the scratch area than cells who didn't shown it. All together these observations suggested that NG2/CSPG4 gave to tumor cells increased opportunities to growth, attached tissue and create masses.

To create metastasis cells should migrate and colonize a new site. So they had to move, change the environment around them and start their trip into the blood and at the end they had to extravasate and colonize a new body district. Our data show that expression of NG2 modulate the capability of cells to extravasate in presence collagen type I, synthetic ECM and native ECM, and. It is known that ECM composition changes from tissue to tissue and that is the motif because the same cell subpopulation show different capability to adhere and migrate on matricies obtained by different cell line: NG2- cells adhered more to MSC ECM that to UTSMC ECM, the opposite happens with NG2+ subpopulation both for sarcoma and melanoma. Probably the different composition of matrix stimulate different pathways involved in adhesion. So we speculate that the adhesion on ECM is a very specific phenomena due to the matrix composition and to its 3D geometry that are peculiar for each

ECM. In order to do a global ECM map we labelled ECM with methabolic labelling: each ECM has a peculiar spatial distribution. The findings highlight a crucial role of sarcoma NG2 in mediating the cells interaction with vascular matrix suggesting its fundamental role in extravasation events and in the tumor cell-endothelium binding.

In perfusion experiments cells enriched by immunosorting for high surface levels of NG2, bound significantly more avidly activated, but not resting, endothelial cells and, most strikingly induced tumor cell clustering in the proximity of the endothelium. NG2+ sarcoma and melanoma cell interaction with the endothelium seem to require the partecipation of the GAG chains of the PG and possibly similar chains on the endothelial cell surface as demonstrated digesting, in two different set of experiments, first endothelia cells and than tumor cell with Chondroitinase ABC. When chondroitin sulfate chains were destroyed cells seemed to lose affinity to activated endothelia. In order to clarified the involvement of NG2/CSPG4 in cell binding we abrogated his expression by siRNA probe on MeWo NG2+ cells and we noticed a strictly correlated with the efficiency of silencing decrease on cell adhesion on activated endothelium: silenced cells adhere 40-50% time less than non abrogated cells. This data shown that NG2/CSPG4, thanks to its complex structure, could be involved in cell adhesion. Antagonists of known cell-cell adhesion molecules and signal transduction probes are now adopted to dissect the involved molecular mechanisms.

We speculate a continuing involvement of this proteoglycan in many cellular pathways and for this motive we started an analysis of gene expression in cell lines that constitutively express different levels of NG2/CSPG4. We discover that 397 genes were modulated only in HT1080 tumor mass, 323 only in MeWo tumor mass and 43 were commonly modulated: some are up-regulated and other are down-regulate.

So we can conclude that NG2/CSPG4 confer a more aggressive phenotype to tumor cells as shown both by *in vitro* experiment and *in vivo* experiments. In fact we tested HT1080 NG2+ ann NG2- cells on CAM assy andour preliminary results shown that HT1080 NG2+ cells were able to pass the CAM barrier and invade embryo chicken organs. Conversely HT1080 NG2- cells migrated on the CAM surface without damaged embryo.

MATERIALS AND METHODS

CELL LINES

Human sarcoma and melanoma cell lines MeWo, HT1080, 143B, A375, and SK-LMS-1 were obtained from ATCC and grown in DMEM (Lonza Walkersville, Maryland, USA) with 10% FBS (Sigma-Aldrich). Uterine Smooth muscle cells (UtSMC) and Mesenchymal Stem Cells (MSC) were obtained by Lonza and grown in SmGM2 medium (Lonza),the Human Umbilical Vein Endothelial cell (HUVEC-Lonza) were grown in M199 medium with 20% and supplemented with bovine brain extract (100µg/ml; Sigma). Endothelia immortalized cells EA.926 hy were obtained by dott. Mongiat Maurizio from CRO of Aviano and grown in DMEM (Lonza Walkersville, Maryland, USA) with 10% FBS (Sigma-Aldrich).

FLOW CYTOMETRY AND CELL SORTING

All flow cytometry measurements were performed on a FACSCalibur (Becton Dickinson) by collecting 10,000 gated events for each sample. A gate was set during acquisition on the forward scatter versus side scatter plot to exclude counting of fragments of deriving from dead cells. Cells were detached from flask using EDTA 5mM and washed twice with sorting Buffer (EDTA 2mM and BSA 0,5% in PBS without calcium and magnesium). Cells were counted (10^7) and re-solubilized in 240µl of buffer and incubated with 60 µl of anti-NG2/CSPG4 mAb 7.1 for 30 minutes at 4°C, than cells were washed in 10 ml of buffer and aliquoted in 3 ml of buffer in a sterile vial. Cells were analyzed with a FACSAria cell sorter II (Becton Dickinson) and the data were anlyazed with the FACSDiva software version 6.1.3. Several controls were performed to determine appropriated gates, voltages, flux and compensation. For the sorting we collected cells in two tubes: A (NG2/CSPG4 +), B (NG2/CSPG4 -). We plated cell and made growth them for some days. Than we analyzed again cells with FACS Calibur: cells were detached from the culture flask using EDTA 5mM and washed twice with PBS and than re-solubilized in PBS at a concentration of 5 x 10^6 cells/ml. A volume of 50µl of cells was incubated for 15 min at RT with 1µl of mouse IgG-PE or 20µl of antibody clone 7.1 + 30µl PBS. Than cells was washed with 2 ml PBS and resuspended in 300µl PBS and analyzed. To test the cell resistance under stress condiction we made the FITC

Annexin V tests (BD Pharmigen^{TM}) after a days of confluence according to the manufactur's data sheet.

CELL PROLIFERATION ASSAY

Cell proliferation was assayed using the Bromodeoxyuridine (BrdU) Cell Proliferation ELISA kit (Roche Diagnostics, Boehringer-Mannheim, Germany), according to manufacturer's instructions. 2.5×10^3 HT1080 immunosorted cells were plated in 96-well flat-bottomed plates and allowed to adhere since confluence and then were starved for 48 hrs. As a control, the same cell subpopulation was maintained in complete medium. After starvation BrdU assay was made.

ANCHORAGE-INDEPENDENT COLONY FORMATION ASSAY

For evaluating anchorage-independent growth, the conventional soft-agar assay was performed using a 1 ml/well bottom layer of 0.8% agar in double-strength Eagle's minimal essential medium containing 10% fetal calf serum, which ws allowed to solidify at room temperature in 6 well microplates. Cells to be tested for colony formation were aliquoted at 2,500 cells/well in a plating layer (1 ml/well) of 0.7% agar in double-strength Eagle's minimal essential medium with 10% fetal calf serum. Cultures were set up in 5 replicates and incubated at 37°C in a humidified incubator in an atmosphere of 5% CO_2 and 95% air. Once to twice per week complete culture medium was added to the wells (0,5 ml/well) and after 7 days wells were stained with 0.5 ml of 0.005% Crystal Violet for more than 1 hr. Cultures were then examined with an inverted phase microscope with x10 and x20 objectives and the final colony counts were made at 6 days after plating for MeWo cells and at 12 days for HT1080 cells.

EVASION ASSAY

For the evaluation of cell evasion, $7.5*10^5$ sarcoma cells were included in Matrigel (6 mg/ml; BD) 10-µl drops, melanoma cells were included in the same matrigel drop with 5% FCS . Cell drops were plated on plastic multiwell plates and after the

matrigel polymerization, complete medium 10% serum was added all around the drops. The evasion ability was estimated 4 days after inclusion photographed using a phase-contrast microscope. Cells outside each drop (5 drops/cell line/experiment) were counted to estimate the evasion ability of each cell line.

TIME-LAPSE MICROSCOPY.

Time-lapse microscopy and scratch analyses were performed in the following way: cells were seeded on plastic and they grown since confluence. Eight hour before starting the test cells were starvated with 0,5% FCS medium, the monolayer was then scratch with a tip and cells were maintained on starvation in order to inhibit cell proliferation and to could test the cell real ability to move. In the next 24 hours we evaluated cell capability to repair the injury so to cover the area cell free created by the scratch. As control we made the same experiment on the same cell line in presence of complete medium.

Pictures were collected every 4 min for 24 h using a charge-coupled-device camera mounted onto the microscope. Collected images were used to create a movie (10 images per second).

TUMORIGENESIS IN MOUSE MODEL

All experiments in mice were approved by the Review Board on animal experimentation of the National Cancer Institute of Aviano and were performed in accordance with the international guidelines for tumorigenesis by xenografting in nude mice. Experiments aimed at assaying tumor formation in relation to NG2 surface expression were performed made a dose-escalation analysis of the number of implanted cells needed to obtain detectable subcutaneous tumor lesions and assayed implantations ranging from 10^6 to $5x10^6$ cells/animal co-injected with Matrigel at a protein concentration of >5 mg/ml.

The study was performed using 10 nude mice subcutaneously inoculated with $5x10^6$ cell immunosorted for NG2/CSPG4. The two subpopulations were injected in one flank and the other one on the other flank. Cells were suspended in Matrigel as described above. In comparative analyses of tumor formation/growth of NG2+

versus NG2- cells, all animals were euthanized at the time that any of subjects manifested signs of morbidity or tumor masses had reached overt sizes of 1.5-2.0 cm^2 in diameter. Euthanized animals were subjected to macroscopical evaluation and photographic documentation of the tumor lesions. During the period of the experiments, care was further taken that the tumor burden did not obviously impair the primary needs of the animals, that is, ambulation, eating, drinking, defecating, and urinating.

WHOLE GENOME DNA MICROARRAY

Total RNA pools was extracted from tumor specimens (≈150mg) and obtained after informed consent using TRIzol Reagent (Invitrogen, Carlsbad CA) and stored at -80°C in RNA secure reagent (Ambion, Inc, Austin TX). RT of mRNA was carried out using High Capacity cDNA Archive kit (Applied Biosystems, Foster City, CA) according to manufacturer's instructions. Gene analysis were made by Human Gene Expression Microarrays Agilent and analyzed with Agilent Software.

Dual Color Microarray-Based Gene Expression Analysis

Wide gene expression analysis of samples has been performed with Microarrays technology. Each Microarray contains sequences representing over 41K human genes and transcripts developed using data sourced from RefSeq, Goldenpath, Ensembl, Unigene, Human Genome Build 33, and others and represents a compiled view of the human genome as it is understood today. Microarrays are an assembly of oligonucleotides fixed on a fine grid of surfaces that allow simultaneous large-scale analysis of thousands of genes at a time. To analyze the expression state of the genes represented in cDNA prepared from mRNA of each examinated tissue sample (expression screening) we have employed Agilent's Dual-Color Microarray-based Gene Expression Analysis. It uses cyanine 3 and cyanine 5-labeled targets to measure gene expression in experimental and control samples Agilent's Quick Amp Labeling Kit generates fluorescent cRNA (complimentary RNA) with a sample input RNA range between 200 ng and 1 µg of total RNA. The method briefly instanced in uses T7 RNA polymerase, which simultaneously amplifies target material and incorporates cyanine 3 and cyanine 5-labeled CTP. . In particular we used cyanine 3

to label cRNA from NG2+ tumor masses and cyanine 5 to labeled cRNA from NG2- tumor masses.

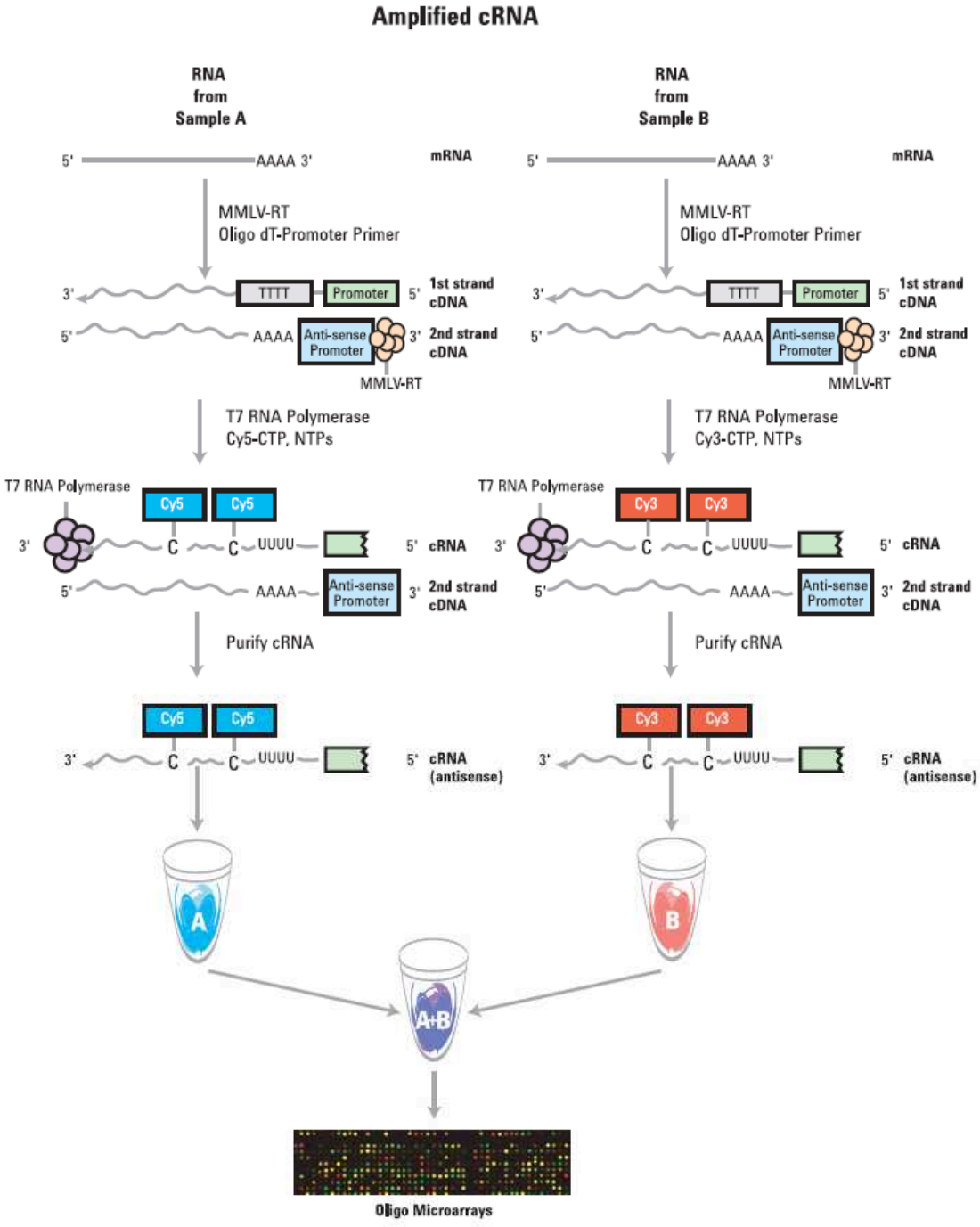

Figure 38- **Schematic of amplified cRNA procedure**. Generation of cRNA for a two-color microarray experiment is shown.

Sample preparation

Dual-Color Spike-Mix Preparation:

Since in gene expression Microarray experiments are multi small differences among samples, procedures or user-induced variations may confound the Microarray data, the Agilent Protocol indicate the use of a positive control to monitor the Agilent Dual-Color Gene Expression Microarray workflow from sample amplification and labeling to Microarray processing. This control is supplied by the Agilent Dual-Color RNA Spike-In Kit and consists of a set of positive control transcripts optimized to anneal to complementary probes on the Microarray with minimal self-hybridization or cross-hybridization. Agilent Dual-Color Microarray experiments with the Agilent Dual-Color RNA Spike-In Kit have been analyzed with the Agilent Feature Extraction software which will generate a QC Report. Tables and graphs from the Agilent QC Report detailed the linear portion of the dynamic range of the Microarray experiment, the high and low detection limits of the experiment, and the reproducibility of the controls with %CV calculations for each of the Spike-In probes. The concentrated Agilent Dual Color RNA Spike-Mix stock was diluted with the Dilution Buffer provided by the kit, then the diluted RNA controls have been spiked directly into the RNA samples and so labeled and amplified together with it. A 5000X Dual-Color Spike-Mix Solution was prepared with Dilution Buffer, then 1 µL of this final dilution was added for every 100 ng of total RNA in the labeling reaction. In our Microarray experiments the initial amount of total RNA always was 500 ng so the 5 µL of Spike-Mix Solution final dilution were added. The final volume of Spike-Mix Solution was mixed with RNA samples.

Purify the labeled/amplified RNA:

Qiagen's RNeasy mini spin columns have been employed for purification of the amplified cRNA samples following manufacturer's instructions. Finally cRNA cleaned samples have been eluted adding 30 µL of RNase-free water directly onto the RNase filter membrane of the spin column and centrifuging al 4°C for 30 seconds at 13000 rpm.

Quantify the cRNA:

Amplified and purified cRNA has been quantified using NanoDrop ND-1000 UV-VIS Spectrophotometer version 3.2.1. The NanoDrop software uses the general form of the Beer-Lambert equation to calculate fluorescent dye concentrations in the Microarray Concentration module.

Hybridization

a) Prepare Hybridization Samples:

Each sample were hybridized using a 4X44K Microarray where four RNA samples can be hybridized at the same time.

The procedure employed was the following:

- Water bath had to be equilibrate to 60°C.
- For each Microarray a Fragmentation mix was prepared adding the components as indicated in table 6 to a 1.5 mL nuclease-free microfuge tube.

Components	Volume/Mass 4x44K	Volume/Mass 8x15K microarrays
cyanine 3-labeled, linearly amplified cRNA	825 ng	300 ng
cyanine 5-labeled, linearly amplified cRNA	825 ng	300 ng
10X Blocking Agent	11 µL	5 µL
Nuclease-free water	bring volume to 52.8 µL	bring volume to 24 µL
25X Fragmentation Buffer	2.2 µL	1 µL
Total Volume	55 µL	25 µL

Table 1- Fragmentation mix for 4x44K Microarrays.

- RNA was fragmented by incubation at 60°C for exactly 30 minutes.
- The appropriate volume (55 µL for 4x44K array format) of 2x GEx Hybridization Buffer HI-RPM was added to stop the fragmentation reaction.
- It was necessary to mix well by careful pipetting, also taking care to avoid introducing bubbles.
- Tubes were spinned for 1 minute at room temperature at 13,000 rpm in a microcentrifuge to drive the sample off the walls and lid and to aid in bubble reduction.

- Samples were placed on ice and immediately loaded onto the array.

Prepare Hybridization Assembly:

- A clean 4 wells gasket slide was placed into the Agilent SureHyb chamber base.
- Slowly 100 µL of hybridization sample were dispensed onto each gasket well in a "drag and dispense" manner.
- Slowly an array "active side" was placed down onto the SureHyb gasket slide.
- The SureHyb chamber cover was placed on the sandwiched slides.
- The assembled hybridization chamber was clamped and placed in rotisserie in an hybridization oven set to 65°C. The hybridization rotator was set to rotate at 10 rpm for 17 hours.

Microarray Wash

The Microarray wash procedure for Agilent's one-color platform had to be done in environments with low ozone level and all dishes, rack and stir bars had to be washed with Milli-Q water. Moreover the addition of 0.005% Triton X-102 to the Gene Expression wash buffers 1 and 2 was performed following the manufacturer's instructions to reduces the possibility to introduce array wash artifacts. Wash conditions are listed in Table 7 and all washes were performed following manufacturer's instructions.

	Dish	Wash Buffer	Temperature	Time
Disassembly	1	GE Wash Buffer 1	Room temperature	
1st wash	2	GE Wash Buffer 1	Room temperature	1 minute
2nd wash	3	GE Wash Buffer 2	Elevated temperature	1 minute

Table 2- **Wash conditions**

Scanning and Feature Extraction

Scan the slides

After the last wash, the slides were placed into the slide holder and scanned immediately to minimize the impact of environmental oxidants on signal intensities. The assembled slide holders was placed into the scanner carousel, the scan settings for Dual-Color scans were verified and
the scanning procedure could be started with the Agilent GenePix 4000B scanner.

Extract data using Agilent Feature Extraction Software

With Feature Extraction (FE) process, the information from probe features were extracted from Microarray scan data, so it was possible to measure genes expression.
Agilent FE 9.5.3 software supports extraction of one-color.tif images of Microarrays scanned on Agilent Scanner and provides at least two important output files to evaluate the performance of the Agilent Microarray system. One is a Microarray image showing visible hybridized Microarray problems, such as wash artifacts and non-visible problems like exposure to Ozone; the other one is a QC report output file which gives information about the accuracy of arrays (reproducibility, signal distribution and background level) (Figure 39).
Moreover, from the acquired high-resolution 16-bit tiff image, raw intensity data are converted in numerical values which are proportional to the fluorescent signal intensity. Thanks to this matrix file containing all the information about each probe (gene name, description, fluorescence intensity), statistical analysis can be performed to have the results of genes expression profiles

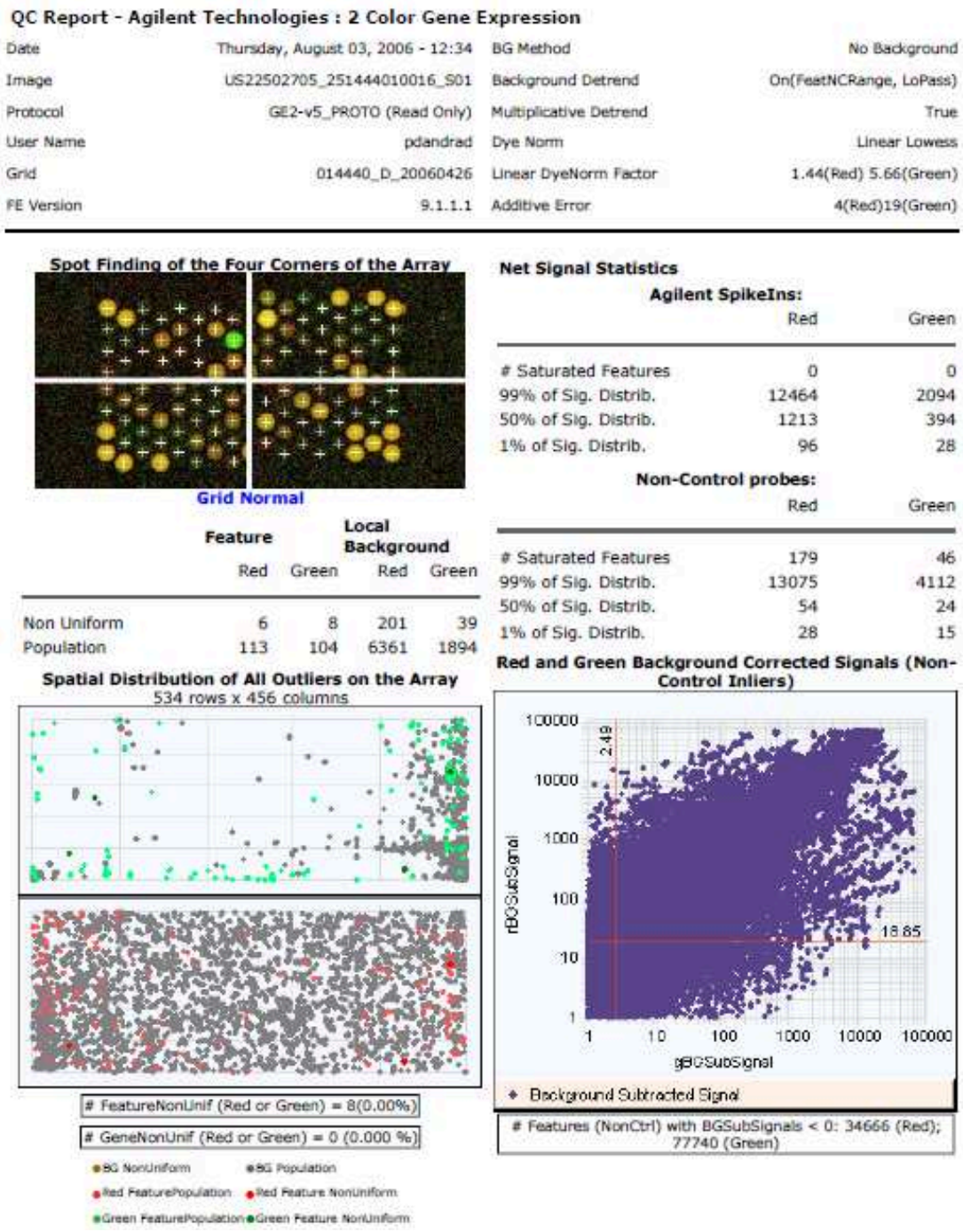

Figure 39- **Example of the first page of a QC Report for 4x44K microarray**, generated by Feature Extraction Softwa

Data analysis

Genes have been classified following their differential expression and then ordered according to their result in the statistical test.

Data have been analyzed performing a software[i] which crosses the results obtained with the information and the accession numbers of genes available on sequence

database (GenBank and EMBL) and finally it completes the panel of information with the GOChart, a usefull image supplied by a tool that identifies ad visualizes enriched GO terms in ranked lists of Human genes where all gene expression heatmap visualizations were generated using Mayday software.

PROTEIN EXTRACTION FROM TUMOR SAMPLES

To perform the protein extraction from tumor semples was used a lysis buffer , the same of Phospho-proteomic profiling described later, composed by:

- 20 mM MOPS, pH 7.0 ;
- 2 mM EGTA (to bind calcium);
- 5 mM EDTA (to bind magnesium and manganese);
- 30 mM sodium fluoride (to inhibit protein-serine phosphatases);
- 60 mM β-glycerophosphate, pH 7.2 (to inhibit protein-serine phosphatases);
- 20 mM sodium pyrophosphate (to inhibit protein-serine phosphatases);
- 1 mM sodium orthovanadate (to inhibit protein-tyrosine phosphatases);
- 1% Triton X-100
- 1 mM phenylmethylsulfonylfluoride (to inhibit proteases);
- 3 mM benzamidine (to inhibit proteases);
- 5 μM pepstatin A (to inhibit proteases);
- 10 μM leupeptin (to inhibit proteases);
- 1 mM dithiothreitol (to reduce disulphide linkages)

The final pH of the buffer was adjusted to 7.2.

For the tissue lyses procedure, briefly: we used 1 ml of lysis buffer per 250 mg wet weight of the chopped tissue. Rinsed the tissue pieces in ice-cold PBS three times to remove blood contaminants, we homogenized the tissue on ice 3 times for 15 seconds each time with a Brinkman Polytron Homogenizer. We sonicated the homogenate 4 times for 10 seconds on ice each time to shear nuclear DNA and centrifuged the sample at 90,000 x g for 30 min at 4°C in a Beckman Table Top TL-

100 ultracentrifuge. Then, we transferred the resulting supernatant fraction to a new tube for protein quantification, using Bradford (Bio-Rad) system by spectrophotometer . Bovine serum albumin (BSA) was used as the protein standard **.**

PHOSPHO-PROTEOMIC PROFILING

The relative expression levels and phosphorylation patterns of signal transduction components elicited by NG2-presence on tumor cell surface was defined by relying upon the Kinetworks^{TM} KAM-1.2PN 300 Phospho-Ab microarrays (Kinexus Bioinformatic Corporation, Vancouver, Canada). The arrays were performed in duplicate using a pool of the same amount of protein-extract deriving from three different tumor masses of same type. Then, the comparison was performed between the two subtypes, NG2+ and NG2- , for each tumor type : HT1080 or MeWo. The results obtained were further compared to exclude the patterns strictly correlated to the melanoma or sarcoma tumor type.

CELL MIGRATION

To examine haptotactic migratory behavior of immunosorted cells on isolated ECM molecules or native ECM, it was performed a classical Transwell assay.

This assay were done using 8-µm pore FALCON HTS FluoroBlock Transwell system (Becton Dickinson) (Figure 1Figure 40). The inserts of the Transwell were coated with the panel of different purified ECM molecules each at the final concentration of 20 ug/ml and ECM were obtained plating cell on transwell membrane and grown them since confluence. After that we put off the ECM extraction protocol. Immunosorted cells were stained with 5 ul/ml of DiI 1mM each $1*10^6$ cells and seeded into the insert at concentration of $5x10^4$ cell/ml/transwell in DMEM with specific % of FBS; the lower chamber contained DMEM 10%. During the next 24 hours from cells seeding it was valued the number of migrated cells through the matrix component using the Inverted Nikon Eclipse TS 100 fluorescent microscope.

The same method were used to test the cell capability to pass through the endothelia: HUVEC cells were growth to obtatined a monolayer on the transwell top, to mimic the extravasation, or to thetranswell bottom to mimic the intravasation.

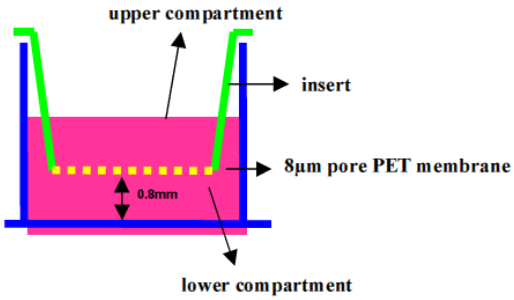

Figure 40: **FALCON HTS FluoroBlock Transwell system.**

ISOLATION OF CELL-FREE NATIVE ECMS

Matrices were isolated from UtSMC,MSC,HUVEC,Wi38,VA-13 either under static or flow-dependent conditions. The cells were grown on glass coverslip for 4-5 days in the presence of 0.25 M ascorbic acid until they reach confluence. Cells were extensively rinsed with Dulbecco's PBS at room temperature and then treated on ice for three periods of 10 minutes according to a procedure modified from Hedman[82]; Nicolosi et al., *in preparation*), using 0.2% sodium deoxycholate (DOC) in 10 mM Tris-Cl buffered saline, pH 8.0, supplemented with a cocktail of proteinases inhibitors including, 4-(2-Aminoethyl) Benzene Sulfonyl Fluoride hydrochloride (AEBSF) 1mM; 6-aminohexanoic acid 5mg/ml; antipain 100 nM; aprotinin 800 nM; chymostatin 100 µM; E-64 10µM; N-ethylamide 1µM; leupeptin 100 µM; pepstatin 1µg/ml (Sigma-Aldrich). Cell dishes were then gently washed 3 times for 10 minutes each on ice with a low ionic strength buffer, 2mM Tris-HCl, pH 8.0, containing the above proteinases inhibitors. Extreme care was taken during pipeting of the solution to avoid detachment of their matrix and to preserve the coverslips on ice. Isolated matrices were visualized by phase-contrast microscopy.

For immunolabelling, samples were fixed in cold methanol (-20°C) for 7 min, washed in PBS and incubated for 15 min at 4°C with blocking solution (PBS 0.1% BSA). Samples were then incubated overnight at 4°C with anti-murine fibronectin

(BD), with an anti-murine Col VI (ABCAM), or anti-human Col I polyclonal antiserum (Millipore Corp.) followed by FITC-conjugated antibody reaction (1 hr at 4°C). Samples were washed three times in PBS and mounted as previously described.

For metabolic labelling we used the kit Click-IT® GalNAz Metabolic Glycoprotein Labeling reagent (Tetraacetylated N-Azidoacetylgalactosamine) by Molecular Probes®.[83]

SDS-PAGE: samples were solubilized in 5X SDS-PAGE loading buffer (250mM, Tris-HCl, pH 6.8, 2.5% SDS; 35% Glycerol, 0.025% (w/v) Bromophenol blue, 125 mM DTT) or 2x sample buffer (4% SDS, 20% Glycerol, 0.12M Tris pH 6.8, and 10% BME) used for SDS-PAGE and resolved on Tris-HCl 5% or pre-cast 4-15% linear gradient gels (Bio-Rad). Precision Plus Protein™ Dual Xtra standards (2–250 kDa), Unstained HiMark Standards (Life Technology Inc.) were employed as molecular markers. Detection was made using the SilverQuest™ Silver Staining Kit according to the) according to manufacturer's protocol.

Purified ECM molecules used as reference were obtained as follows: human fibronectin, collagen type I from bovine achilles tendon collagen type III, tetrameric collagen type IV, collagen type VI and vitronectin from Sigma-Aldrich; rat tail Col I and matrigel from BD Biosciences; dimeric mouse collagen type IV from Merck Laboratories-Collaborative Research. For substrate coating, ECM components were diluted in 0.05 M bicarbonate buffer, pH 9.6, and coated at the final concentration of 20 μg/ml overnight at 4°C in a moist chamber.

For isolation of cell-free ECMs under flow cells were seeded at high density (from 3 to $5x10^5$ cells depending on cells type) onto sterile coverslips (25x50 mm), such as to obtain a confluent monolayer the following day. Cells were then further cultivated for up to 5 days. To avoid delays in the washing step at time of ECM isolation, 1 ml of "washing buffer" was flushed into the liquid-bearing tube before its insertion into the perfusion chamber and this latter was then assembled[84]. The cell "lysis solution" was next gently injected into the perfusion chamber and allowed to come in contact with the cells for 90 sec. The tubing containing the "washing buffer" was connected to a syringe pump (Harvard Scientifics Inc) which was set at a share rate of $25s^{-1}$. The isolation procedure was monitored by phase-contrast microscopy and topology and integrity of the isolated matrices contained within the perfusion chamber was verified by immunostaining for FN. Analysis of cell-matrix interactions

under defined shear-rates was performed according to previously described procedures.[85]

CELL ADHESION ASSAYS UNDER PERFUSION

After the isolation of cell-free matrices under perfusion, perfused cells (stained before with 5 ul/ml of DiI 1mM each $1*10^6$ cells) were re-suspended at final concentration of $1x10^6$ cells/ml in M199 medium supplemented with 0% FCS. A volume of 1.5 ml of the cell suspension was used for each perfusion. To made our experiment we used a perfusion system describe above (figure 10). The shear rate was set at 25 s^{-1} and the perfused cells were recorded by capturing 20 random fields on each coverslip at 5 and 10 min after the beginning of the perfusion.

For perfusion assay HUVEC cells and EA926.hy cells were seeded on glass cover slip and grown to obtain a omogeneus monolayer each with the specific medium. Four hours before the perfusion experiments cells were put in an activation medium made with 0% FCS and TNFα (10-20 ng/ml). As control we used the same cell lines treated for the same time in 0% FCS medium only. After endothelia activation time perfused cells (stained before with 5 ul/ml of DiI 1mM each $1*10^6$ cells) were re-suspended at final concentration of $1x10^6$ cells/ml in M199 medium supplemented with 0% FCS. The flow experiment was conducted at 50 sec^{-1} shear rate and cell adhesion and aggregation were monitoreted each 5 minutes for 10 minutes.

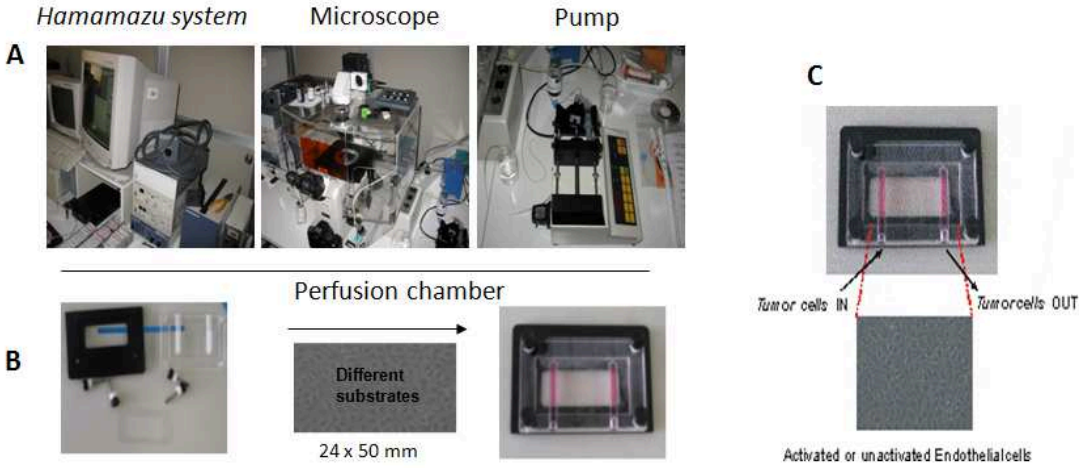

Figure 41- **Perfusion system:** (A) Left: recording system with a high-resolution CCD camera to study the kinetics of cellular and subcellular events taking place under defined flow rates (shear forces); center: inverted microscopy to follow the experiment in contrast phase or with fluorescence lamp. Right: peristaltic pump to modulate and change the share rate to mimic physiological condition of blood and lymphatic vessels. (B) Perfusion chamber: on a metallic support is possible put a rectangular coverslip with cells to obtain a close system to analyze them in different condition on flow dynamic. (C) Perfusion chamber dynamics: the transparent chamber gives the possibility to follow the experiment under the microscope and follow the dynamics on different substrates over the coverslip . It presents a entrance of the fluid (with the tumor cells in perfusion) and a exit.

To discriminate and count cell on flow we set up a new softwear thanks to the collaboration between Dott. Elisabetta Lombardi and Ing. Leonardo Buscemi. The softwear, called Cell Counter-BL, exploits the characteristics of long exposure photographs in which the moving parts tend to disappear, while the elements properties are imprinted on the image , the same way the cells are still seen as the mobile ones do not.

DETAIL : Simply by making a sum of the frames that constitute a field of view and dividing by the number of frames is obtained a similar effect to a long exposures. The starting image have a background illumination is inhomogeneous , because of presence of a bright spot , the point of making the background brighter than the central area to a suburban area with adherent cell . For this reason it was necessary to perform a background subtraction with a calculation of the dynamic background on each image . It was used interpolating function of degree 4 for all rows of the image.For the part of the cell count has exploited an algorithm known in the literature (http://en.wikipedia.org/wiki/Flood_fill).

In all experiments of adhesion and migration was applied as statistical test the *Student't*-test to determine the statistical significance of differences between means

of three independent experiments, each in triplicate. Significance was defined as a $P<0.5$; $P<0.05$; $P<0.005$.

RNAi-MEDIATED NG2/CSPG4 ABROGATION

siRNA probes against NG2 , and scrambled versions of these probes were obtained through Ambion (Austin, TX). Transfections were performed by using siLentFect Lipid Reagent (Bio-RAD) according to manufacturer's protocol. The optimal siRNA concentration was observed at 20nM and 3µl/ml of siLentFect Reagent. For each well to be trasfected (12 well plate) was prepared 50µl of serum free-medium containing 3µl of siLentFect Reagent , and, separately, 50µl of serum free-medium containing the siRNA. The two solution were mixed and incubated for 20 minutes at room temperature. Then the mix was added directly to cells (70 % confluence) in complete medium. Relative levels of expression siRNA knock-down NG2/CSPG4, were determined at by FACS and immunoblotting (Cattaruzza et al., 2012)

CAM ASSAY

Fertilized chicken eggs were incubated at 38°C at constant humidity. On third day of incubation a square window was opened in the eggs shell after suction of 2-3 ml of albumen so as to detach the developing CAM from the shell. The window was closed and eggs were returned into the incubator. On eight day of incubation, $4x10^5$ cells were resuspended in Matrigel and seeded on the top of a growing CAM. After 72-96 hours, the angiogenic response of the implants was evaluated through a stereomicroscope equipped with a CCD camera (Nikon, Italia). After embryos sacrifice, samples from internal organs (liver, lungs and brain) and from CAM (proximal and distal site from the inoculum) were recovered. All samples were stored at -80°C for molecular analysis. For identification of disseminated human cancer cells in the chick embryo we used amplification of human ALU sequences. To this end the purification of chicken-human DNA samples was performed using Spin-Column Protocol by QIAGEN. The thus purified DNA was quantified with a spectrophotometer at 595 nm. PCR was performed using the following primers:

Forward ACGCCTGTAATCCCAGCACTT and Reverse TCGCCCAGGCTGGAGTGCA. The conditions in which PCR was performed were: denaturation at 95°C for 30 min, annealing at 60°C at 30 min, elongation at 72°C for 30' min for 30 cycles. The amount of DNA loaded was 100 ng. The amplification product (244bp of length) was displayed with 1,8% agarose gel electrophoresis in TAE Buffer. The image of gel was collected by AlphaImager instrument.

For identification of cells through immunohistochemistry, cryosections of chicken CAM and chicken internal organs (brain, liver, lung) were treated with methanol and 3% H_2O_2 for 15 min, and goat serum for 20 min before incubating with a monoclonal mouse antibody direct against the human nuclear antigen NuMA (1:250 v/v) for 2 h at room temperature. Immunoreactions were revealed with DAKO HRP Advance system and diaminobenzidine (DAB) (DAKO, Hamburg, Germany).

BIBLIOGRAPHY

1. Chiang, A. C. & Massagué, J. Molecular basis of metastasis. *N. Engl. J. Med.* **359,** 2814–2823 (2008).
2. Nguyen, D. X. *et al.* WNT/TCF signaling through LEF1 and HOXB9 mediates lung adenocarcinoma metastasis. *Cell* **138,** 51–62 (2009).
3. Valastyan, S. & Weinberg, R. A. Tumor metastasis: molecular insights and evolving paradigms. *Cell* **147,** 275–292 (2011).
4. Reymond, N., d' Água, B. B. & Ridley, A. J. Crossing the endothelial barrier during metastasis. *Nat. Rev. Cancer* **13,** 858–870 (2013).
5. Wyckoff, J. B., Jones, J. G., Condeelis, J. S. & Segall, J. E. A critical step in metastasis: in vivo analysis of intravasation at the primary tumor. *Cancer Res.* **60,** 2504–2511 (2000).
6. Kedrin, D., Wyckoff, J., Sahai, E., Condeelis, J. & Segall, J. E. Imaging tumor cell movement in vivo. *Curr. Protoc. Cell Biol. Editor. Board Juan Bonifacino Al* **Chapter 19,** Unit 19.7 (2007).
7. Sahai, E. & Marshall, C. J. Differing modes of tumour cell invasion have distinct requirements for Rho/ROCK signalling and extracellular proteolysis. *Nat. Cell Biol.* **5,** 711–719 (2003).
8. Friedl, P. & Gilmour, D. Collective cell migration in morphogenesis, regeneration and cancer. *Nat. Rev. Mol. Cell Biol.* **10,** 445–457 (2009).
9. Lowe, K. L., Navarro-Nunez, L. & Watson, S. P. Platelet CLEC-2 and podoplanin in cancer metastasis. *Thromb. Res.* **129 Suppl 1,** S30–37 (2012).
10. Kienast, Y. *et al.* Real-time imaging reveals the single steps of brain metastasis formation. *Nat. Med.* **16,** 116–122 (2010).
11. Stoletov, K. *et al.* Visualizing extravasation dynamics of metastatic tumor cells. *J. Cell Sci.* **123,** 2332–2341 (2010).
12. Ito, S. *et al.* Tumor promoting effect of podoplanin-positive fibroblasts is mediated by enhanced RhoA activity. *Biochem. Biophys. Res. Commun.* **422,** 194–199 (2012).
13. Ley, K., Laudanna, C., Cybulsky, M. I. & Nourshargh, S. Getting to the site of inflammation: the leukocyte adhesion cascade updated. *Nat. Rev. Immunol.* **7,** 678–689 (2007).
14. Strell, C. & Entschladen, F. Extravasation of leukocytes in comparison to tumor cells. *Cell Commun. Signal. CCS* **6,** 10 (2008).
15. Mook, O. R. F. *et al.* Visualization of early events in tumor formation of eGFP-transfected rat colon cancer cells in liver. *Hepatol. Baltim. Md* **38,** 295–304 (2003).
16. Hiratsuka, S. *et al.* Endothelial focal adhesion kinase mediates cancer cell homing to discrete regions of the lungs via E-selectin up-regulation. *Proc. Natl. Acad. Sci. U. S. A.* **108,** 3725–3730 (2011).
17. Köhler, S., Ullrich, S., Richter, U. & Schumacher, U. E-/P-selectins and colon carcinoma metastasis: first in vivo evidence for their crucial role in a clinically relevant model of spontaneous metastasis formation in the lung. *Br. J. Cancer* **102,** 602–609 (2010).
18. Miles, F. L., Pruitt, F. L., van Golen, K. L. & Cooper, C. R. Stepping out of the flow: capillary extravasation in cancer metastasis. *Clin. Exp. Metastasis* **25,** 305–324 (2008).

19. Shirure, V. S., Reynolds, N. M. & Burdick, M. M. Mac-2 binding protein is a novel E-selectin ligand expressed by breast cancer cells. *PloS One* **7,** e44529 (2012).
20. Läubli, H. & Borsig, L. Selectins promote tumor metastasis. *Semin. Cancer Biol.* **20,** 169–177 (2010).
21. St Hill, C. A. Interactions between endothelial selectins and cancer cells regulate metastasis. *Front. Biosci. Landmark Ed.* **16,** 3233–3251 (2011).
22. Barthel, S. R. *et al.* Definition of molecular determinants of prostate cancer cell bone extravasation. *Cancer Res.* **73,** 942–952 (2013).
23. Felding-Habermann, B. *et al.* Integrin activation controls metastasis in human breast cancer. *Proc. Natl. Acad. Sci. U. S. A.* **98,** 1853–1858 (2001).
24. Felding-Habermann, B., Habermann, R., Saldívar, E. & Ruggeri, Z. M. Role of beta3 integrins in melanoma cell adhesion to activated platelets under flow. *J. Biol. Chem.* **271,** 5892–5900 (1996).
25. Laferrière, J., Houle, F. & Huot, J. Adhesion of HT-29 colon carcinoma cells to endothelial cells requires sequential events involving E-selectin and integrin beta4. *Clin. Exp. Metastasis* **21,** 257–264 (2004).
26. Kawakami-Kimura, N. *et al.* Involvement of hepatocyte growth factor in increased integrin expression on HepG2 cells triggered by adhesion to endothelial cells. *Br. J. Cancer* **75,** 47–53 (1997).
27. Orian-Rousseau, V. CD44, a therapeutic target for metastasising tumours. *Eur. J. Cancer Oxf. Engl. 1990* **46,** 1271–1277 (2010).
28. Zen, K. *et al.* CD44v4 is a major E-selectin ligand that mediates breast cancer cell transendothelial migration. *PloS One* **3,** e1826 (2008).
29. Draffin, J. E., McFarlane, S., Hill, A., Johnston, P. G. & Waugh, D. J. J. CD44 potentiates the adherence of metastatic prostate and breast cancer cells to bone marrow endothelial cells. *Cancer Res.* **64,** 5702–5711 (2004).
30. Mine, S. *et al.* Hepatocyte growth factor enhances adhesion of breast cancer cells to endothelial cells in vitro through up-regulation of CD44. *Exp. Cell Res.* **288,** 189–197 (2003).
31. Okado, T. & Hawley, R. G. Adhesion molecules involved in the binding of murine myeloma cells to bone marrow stromal elements. *Int. J. Cancer J. Int. Cancer* **63,** 823–830 (1995).
32. Fujisaki, T. *et al.* CD44 stimulation induces integrin-mediated adhesion of colon cancer cell lines to endothelial cells by up-regulation of integrins and c-Met and activation of integrins. *Cancer Res.* **59,** 4427–4434 (1999).
33. Wang, H.-S. *et al.* CD44 cross-linking induces integrin-mediated adhesion and transendothelial migration in breast cancer cell line by up-regulation of LFA-1 (alpha L beta2) and VLA-4 (alpha4beta1). *Exp. Cell Res.* **304,** 116–126 (2005).
34. Cattaruzza, S. & Perris, R. Proteoglycan control of cell movement during wound healing and cancer spreading. *Matrix Biol. J. Int. Soc. Matrix Biol.* **24,** 400–417 (2005).
35. Garusi, E., Rossi, S. & Perris, R. Antithetic roles of proteoglycans in cancer. *Cell. Mol. Life Sci. CMLS* **69,** 553–579 (2012).
36. Whiteford, J. R. *et al.* Syndecans promote integrin-mediated adhesion of mesenchymal cells in two distinct pathways. *Exp. Cell Res.* **313,** 3902–3913 (2007).
37. Morgan, M. R., Humphries, M. J. & Bass, M. D. Synergistic control of cell adhesion by integrins and syndecans. *Nat. Rev. Mol. Cell Biol.* **8,** 957–969 (2007).

38. Sanderson, R. D., Turnbull, J. E., Gallagher, J. T. & Lander, A. D. Fine structure of heparan sulfate regulates syndecan-1 function and cell behavior. *J. Biol. Chem.* **269,** 13100–13106 (1994).
39. Kato, M., Wang, H., Bernfield, M., Gallagher, J. T. & Turnbull, J. E. Cell surface syndecan-1 on distinct cell types differs in fine structure and ligand binding of its heparan sulfate chains. *J. Biol. Chem.* **269,** 18881–18890 (1994).
40. Lebakken, C. S., McQuade, K. J. & Rapraeger, A. C. Syndecan-1 signals independently of beta1 integrins during Raji cell spreading. *Exp. Cell Res.* **259,** 315–325 (2000).
41. Hoffman, M. P. *et al.* Laminin-1 and laminin-2 G-domain synthetic peptides bind syndecan-1 and are involved in acinar formation of a human submandibular gland cell line. *J. Biol. Chem.* **273,** 28633–28641 (1998).
42. Yokoyama, F. *et al.* Bifunctional peptides derived from homologous loop regions in the laminin alpha chain LG4 modules interact with both alpha 2 beta 1 integrin and syndecan-2. *Biochemistry (Mosc.)* **44,** 9581–9589 (2005).
43. Hozumi, K., Suzuki, N., Nielsen, P. K., Nomizu, M. & Yamada, Y. Laminin alpha1 chain LG4 module promotes cell attachment through syndecans and cell spreading through integrin alpha2beta1. *J. Biol. Chem.* **281,** 32929–32940 (2006).
44. Bachy, S., Letourneur, F. & Rousselle, P. Syndecan-1 interaction with the LG4/5 domain in laminin-332 is essential for keratinocyte migration. *J. Cell. Physiol.* **214,** 238–249 (2008).
45. Adams, J. C., Kureishy, N. & Taylor, A. L. A role for syndecan-1 in coupling fascin spike formation by thrombospondin-1. *J. Cell Biol.* **152,** 1169–1182 (2001).
46. Beauvais, D. M. & Rapraeger, A. C. Syndecan-1-mediated cell spreading requires signaling by alphavbeta3 integrins in human breast carcinoma cells. *Exp. Cell Res.* **286,** 219–232 (2003).
47. Beauvais, D. M., Ell, B. J., McWhorter, A. R. & Rapraeger, A. C. Syndecan-1 regulates alphavbeta3 and alphavbeta5 integrin activation during angiogenesis and is blocked by synstatin, a novel peptide inhibitor. *J. Exp. Med.* **206,** 691–705 (2009).
48. Lambaerts, K., Wilcox-Adelman, S. A. & Zimmermann, P. The signaling mechanisms of syndecan heparan sulfate proteoglycans. *Curr. Opin. Cell Biol.* **21,** 662–669 (2009).
49. Wang, Z. *et al.* RGD-independent cell adhesion via a tissue transglutaminase-fibronectin matrix promotes fibronectin fibril deposition and requires syndecan-4/2 α5β1 integrin co-signaling. *J. Biol. Chem.* **285,** 40212–40229 (2010).
50. Park, H., Kim, Y., Lim, Y., Han, I. & Oh, E.-S. Syndecan-2 mediates adhesion and proliferation of colon carcinoma cells. *J. Biol. Chem.* **277,** 29730–29736 (2002).
51. Choi, Y. *et al.* Syndecan-2 regulates cell migration in colon cancer cells through Tiam1-mediated Rac activation. *Biochem. Biophys. Res. Commun.* **391,** 921–925 (2010).
52. Vuoriluoto, K., Högnäs, G., Meller, P., Lehti, K. & Ivaska, J. Syndecan-1 and -4 differentially regulate oncogenic K-ras dependent cell invasion into collagen through α2β1 integrin and MT1-MMP. *Matrix Biol. J. Int. Soc. Matrix Biol.* **30,** 207–217 (2011).
53. Araki, E. *et al.* Clustering of syndecan-4 and integrin beta1 by laminin alpha 3 chain-derived peptide promotes keratinocyte migration. *Mol. Biol. Cell* **20,** 3012–3024 (2009).
54. Stepp, M. A. *et al.* Syndecan-1 regulates cell migration and fibronectin fibril assembly. *Exp. Cell Res.* **316,** 2322–2339 (2010).

55. Ishikawa, T. & Kramer, R. H. Sdc1 negatively modulates carcinoma cell motility and invasion. *Exp. Cell Res.* **316,** 951–965 (2010).
56. Langford, J. K. & Sanderson, R. D. Measurements of glycosaminoglycan-based cell interactions. *Methods Cell Biol.* **69,** 297–308 (2002).
57. Liebersbach, B. F. & Sanderson, R. D. Expression of syndecan-1 inhibits cell invasion into type I collagen. *J. Biol. Chem.* **269,** 20013–20019 (1994).
58. Yang, R. Y., Hill, P. N., Hsu, D. K. & Liu, F. T. Role of the carboxyl-terminal lectin domain in self-association of galectin-3. *Biochemistry (Mosc.)* **37,** 4086–4092 (1998).
59. Wilcox-Adelman, S. A., Denhez, F. & Goetinck, P. F. Syndecan-4 modulates focal adhesion kinase phosphorylation. *J. Biol. Chem.* **277,** 32970–32977 (2002).
60. Munesue, S. *et al.* The role of syndecan-2 in regulation of actin-cytoskeletal organization of Lewis lung carcinoma-derived metastatic clones. *Biochem. J.* **363,** 201–209 (2002).
61. Langford, D., Hurford, R., Hashimoto, M., Digicaylioglu, M. & Masliah, E. Signalling crosstalk in FGF2-mediated protection of endothelial cells from HIV-gp120. *BMC Neurosci.* **6,** 8 (2005).
62. Ridgway, L. D., Wetzel, M. D. & Marchetti, D. Modulation of GEF-H1 induced signaling by heparanase in brain metastatic melanoma cells. *J. Cell. Biochem.* **111,** 1299–1309 (2010).
63. Cattaruzza, S. *et al.* NG2/CSPG4-collagen type VI interplays putatively involved in the microenvironmental control of tumour engraftment and local expansion. *J. Mol. Cell Biol.* **5,** 176–193 (2013).
64. Majumdar, M., Vuori, K. & Stallcup, W. B. Engagement of the NG2 proteoglycan triggers cell spreading via rac and p130cas. *Cell. Signal.* **15,** 79–84 (2003).
65. Midwood, K. S. & Salter, D. M. Expression of NG2/human melanoma proteoglycan in human adult articular chondrocytes. *Osteoarthr. Cartil. OARS Osteoarthr. Res. Soc.* **6,** 297–305 (1998).
66. Garrigues, H. J. *et al.* The melanoma proteoglycan: restricted expression on microspikes, a specific microdomain of the cell surface. *J. Cell Biol.* **103,** 1699–1710 (1986).
67. Wilson, B. S., Ruberto, G. & Ferrone, S. Immunochemical characterization of a human high molecular weight--melanoma associated antigen identified with monoclonal antibodies. *Cancer Immunol. Immunother. CII* **14,** 196–201 (1983).
68. Pouly, S., Becher, B., Blain, M. & Antel, J. P. Expression of a homologue of rat NG2 on human microglia. *Glia* **27,** 259–268 (1999).
69. Mangieri, D. *et al.* Angiogenic activity of multiple myeloma endothelial cells in vivo in the chick embryo chorioallantoic membrane assay is associated to a down-regulation in the expression of endogenous endostatin. *J. Cell. Mol. Med.* **12,** 1023–1028 (2008).
70. Schlingemann, R. O., Rietveld, F. J., de Waal, R. M., Ferrone, S. & Ruiter, D. J. Expression of the high molecular weight melanoma-associated antigen by pericytes during angiogenesis in tumors and in healing wounds. *Am. J. Pathol.* **136,** 1393–1405 (1990).
71. Pujana, M. A. *et al.* Additional complexity on human chromosome 15q: identification of a set of newly recognized duplicons (LCR15) on 15q11-q13, 15q24, and 15q26. *Genome Res.* **11,** 98–111 (2001).
72. Campoli, M. R. *et al.* Human high molecular weight-melanoma-associated antigen (HMW-MAA): a melanoma cell surface chondroitin sulfate proteoglycan

(MSCP) with biological and clinical significance. *Crit. Rev. Immunol.* **24,** 267–296 (2004).
73. Ross, A. H. *et al.* Isolation and chemical characterization of a melanoma-associated proteoglycan antigen. *Arch. Biochem. Biophys.* **225,** 370–383 (1983).
74. Stallcup, W. B. The NG2 proteoglycan: past insights and future prospects. *J. Neurocytol.* **31,** 423–435 (2002).
75. Stallcup, W. B. & Huang, F.-J. A role for the NG2 proteoglycan in glioma progression. *Cell Adhes. Migr.* **2,** 192–201 (2008).
76. Price, M. A. *et al.* CSPG4, a potential therapeutic target, facilitates malignant progression of melanoma. *Pigment Cell Melanoma Res.* **24,** 1148–1157 (2011).
77. Joo, N. E. *et al.* NG2, a novel proapoptotic receptor, opposes integrin alpha4 to mediate anoikis through PKCalpha-dependent suppression of FAK phosphorylation. *Cell Death Differ.* **15,** 899–907 (2008).
78. Cattaruzza, S. *et al.* NG2/CSPG4-collagen type VI interplays putatively involved in the microenvironmental control of tumour engraftment and local expansion. *J. Mol. Cell Biol.* **5,** 176–193 (2013).
79. Campoli, M., Ferrone, S. & Wang, X. Functional and clinical relevance of chondroitin sulfate proteoglycan 4. *Adv. Cancer Res.* **109,** 73–121 (2010).
80. Cattaruzza, S. *et al.* Multivalent proteoglycan modulation of FGF mitogenic responses in perivascular cells. *Angiogenesis* **16,** 309–327 (2013).
81. Schlingemann, R. O. *et al.* Differential expression of markers for endothelial cells, pericytes, and basal lamina in the microvasculature of tumors and granulation tissue. *Am. J. Pathol.* **138,** 1335–1347 (1991).
82. Hedman, K. *et al.* Isolation of the pericellular matrix of human fibroblast cultures. *J. Cell Biol.* **81,** 83–91 (1979).
83. Laughlin, S. T. *et al.* Metabolic labeling of glycans with azido sugars for visualization and glycoproteomics. *Methods Enzymol.* **415,** 230–250 (2006).
84. Munn, L. L., Melder, R. J. & Jain, R. K. Analysis of cell flux in the parallel plate flow chamber: implications for cell capture studies. *Biophys. J.* **67,** 889–895 (1994).
85. Mazzucato, M. *et al.* Distinct spatio-temporal Ca2+ signaling elicited by integrin alpha2beta1 and glycoprotein VI under flow. *Blood* **114,** 2793–2801 (2009).
86. Chang, K. C., Tees, D. F. & Hammer, D. A. The state diagram for cell adhesion under flow: leukocyte rolling and firm adhesion. *Proc. Natl. Acad. Sci. U. S. A.* **97,** 11262–11267 (2000).
87. Rozario, T. & DeSimone, D. W. The extracellular matrix in development and morphogenesis: a dynamic view. *Dev. Biol.* **341,** 126–140 (2010).
88. Bouïs, D., Hospers, G. A., Meijer, C., Molema, G. & Mulder, N. H. Endothelium in vitro: a review of human vascular endothelial cell lines for blood vessel-related research. *Angiogenesis* **4,** 91–102 (2001).
89. Eisenmann, K. M. *et al.* Melanoma chondroitin sulphate proteoglycan regulates cell spreading through Cdc42, Ack-1 and p130cas. *Nat. Cell Biol.* **1,** 507–513 (1999).
90. Chatterjee, N. *et al.* Interaction of syntenin-1 and the NG2 proteoglycan in migratory oligodendrocyte precursor cells. *J. Biol. Chem.* **283,** 8310–8317 (2008).